Theory of Extremely Correlated Fermions (III-IV)

Sriram Shastry
University of California
Santa Cruz, CA

Collège de France
April 9 2014

Work supported by
DOE, BES DE-FG02-06ER46319

Lightening Summary of last lecture

Usual Dyson type theory

$$\mathcal{G}(k,i\omega) \to \underbrace{\frac{1-\frac{n}{2}}{i\omega+\mu-c\,\varepsilon_k-\Sigma(k,i\omega)}}_{Dyson form}$$

ECFL form gives instead:

$$\mathcal{G}(k,i\omega) = \underbrace{\frac{1}{i\omega+\mu-c\varepsilon_k-\Phi(k,i\omega)}}_{g(k,i\omega)} \times \underbrace{[1-\frac{n}{2}+\Psi(k,i\omega)]}_{\mu(k,i\omega)}$$

auxiliary Greens function

caparison function

- Calculation of the two self energies proceeds by one of three methods.
  - Expansion in parameter λ analogous to 1/(2S) in spin wave theory, by a self consistent skeleton graph expansion (numerically implemented). Formulas for self energies look like bubble graphs in Fermi liquid theory- self consistently lead to FL type behaviour
  - Phenomenological models for Ψ and Φ based on Fermi liquid type hypothesis from the λ expansion
  - Low k,ω expansion of the self energies Ψ and Φ, inspired by the comparison with DMFT-

$$\Psi(k) = -2\lambda\sum_{p,q} E(k,p)\mathbf{g}(p)\mathbf{g}(q)\mathbf{g}(q+p-k),$$

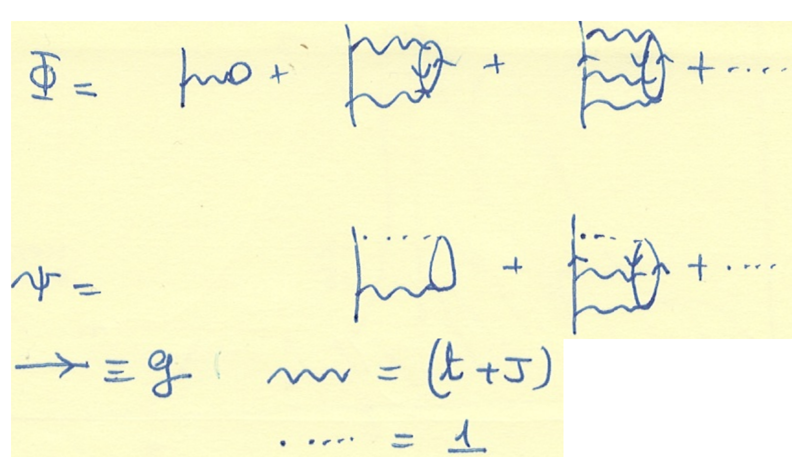

$$\bar{\Phi}(k) = -2\lambda\sum_{p,q} E(k,p)[E(p,k)+E(q+p-k,p)] \times \mathbf{g}(p)\mathbf{g}(q)\mathbf{g}(q+p-k).$$

Phenomenological spectral function s-ECFL
(Shastry PRL 2011, Gweon et al PRL 2011)

$$\Psi(\omega) \sim -\frac{1}{\Delta}\Phi(\omega)$$

Dimensional/engineering approximation of $O(\lambda^2)$ equations.

$$\Phi(\omega) = \int dx \frac{\Gamma(x)}{i\omega - x}$$

$$\Gamma(\omega) = \frac{\omega^2 + \pi^2 T^2}{\omega_0} e^{-(\pi^2 T^2 + \omega^2)/\Omega_0^2}$$

$$h(\omega) = \mathcal{P} \int \frac{\Gamma(\omega')}{(\omega - \omega')} d\omega' = \text{error function}$$

$$A_{FL}(\omega) = \frac{\Gamma(\omega)}{\Gamma^2(\omega) + (\omega - \hat{k}v_F - h(\omega))^2}$$

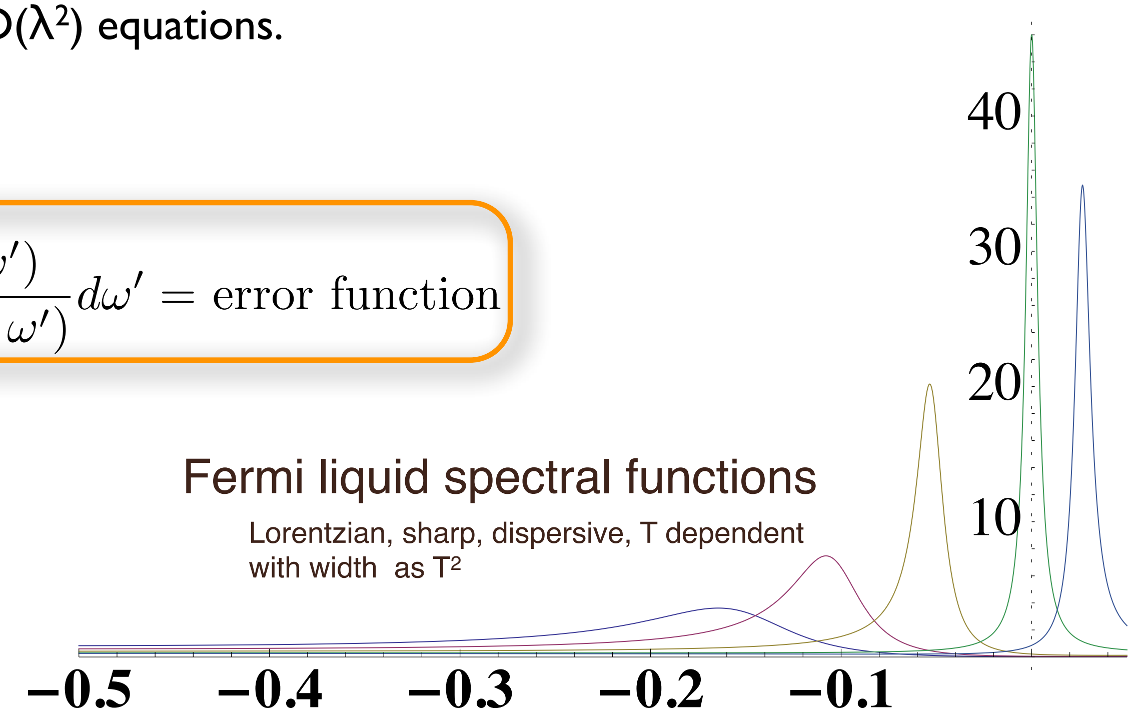

Fermi liquid spectral functions

Lorentzian, sharp, dispersive, T dependent with width as T^2

$$A_{sECFL}(\omega) = \frac{1}{\pi} \frac{\Gamma(\omega)}{\Gamma^2(\omega) + (\omega - \hat{k}v_F - h(\omega))^2} \times (1 - \frac{\omega}{\Delta} + c\hat{k}v_F)$$

Remarkably light description
with only three parameters: (c is fixed, Δ computed).
1) η (Impurity scattering- extrinsic) so that $\Gamma \to \Gamma + \eta$.
(needed for Laser vs synchrotron ARPES)
2) Ω_0 (strength of FL)
3) ω_0 (High frequncy cut off of FL)

$$\Delta = \int d\omega f(\omega) \langle A_{FL}(k,\omega)(\epsilon - \mu - \omega)\rangle_k$$

Expand both the self energies at small (k, ω) assuming a Fermi liquid structure.

Long wavelength expansion

$$1-\frac{n}{2}+\Psi(\vec{k},\omega)=\alpha_0+c_\Psi(\omega+\nu_\Psi\,\hat{k}\,v_f)+i\mathcal{R}/\gamma_\Psi+O(\omega^3)$$

$$\omega+\boldsymbol{\mu}-\left(1-\frac{n}{2}\right)\varepsilon_k-\Phi(k,\omega)=(1+c_\Phi)\left(\omega-\nu_\Phi\,\hat{k}\,v_f+i\mathcal{R}/\Omega_\Phi+O(\omega^3)\right)$$

$$\mathcal{R}=\pi\{\omega^2+(\pi k_BT)^2\}$$

$$\hat{k}\;=\;(\vec{k}-\vec{k}_F).\vec{k}_F/|\vec{k}_F|$$

$v_f\;=\;(\partial_k\varepsilon_k)_{k_F}$ is the *bare* Fermi velocity

$$\alpha_0=1-\frac{n}{2}+\Psi_0\rightarrow(1-n)$$

Non Lorentzian Spectral function with 5 parameters

$$A(\vec{k},\omega)=\frac{z_0}{\pi}\frac{\Gamma_0}{(\omega-\nu_\Phi\,\hat{k}\,v_f)^2+\Gamma_0^2}\times\mu(k,\omega)$$

$$\Gamma_0(\hat{k},\omega)=\eta+\frac{\pi(\omega^2+(\pi k_BT)^2)}{\Omega_\Phi}$$

$$\mu(\hat{k},\omega)=1-\frac{\omega}{\Delta_0}+\frac{\nu_0\,\hat{k}\,v_f}{\Delta_0}$$

$\{\Delta_0,z_0,\Omega_\Phi,\nu_0,\nu_\Phi\}$ $\quad v_F\rightarrow$ bare Fermi velocity

Comments:

- Notable feature of all the ECFL spectral functions is the non Lorentzian nature- due to the multiplying factor (caparison factor) that depends on k and ω.
- As a result different "spectra"- locating the maxima of A(k,ω)-are definable:
    - at fixed k scan various ω (EDC's)
    - at fixed ω scan versus k (MDC's)
- The MDC spectrum and EDC spectrum differ at very low energies in the spectral function $A_{ECFL}(k,\omega)$- the caparison factor makes the difference.
- The story has a parallel in neutron scattering,   See- *the notorious case of spin waves in Iron above Tc*, (1978-81).
- Here locating *spin waves* from constant k scans is right, often constant ω scans were used to make dramatic, but ultimately incorrect claims.

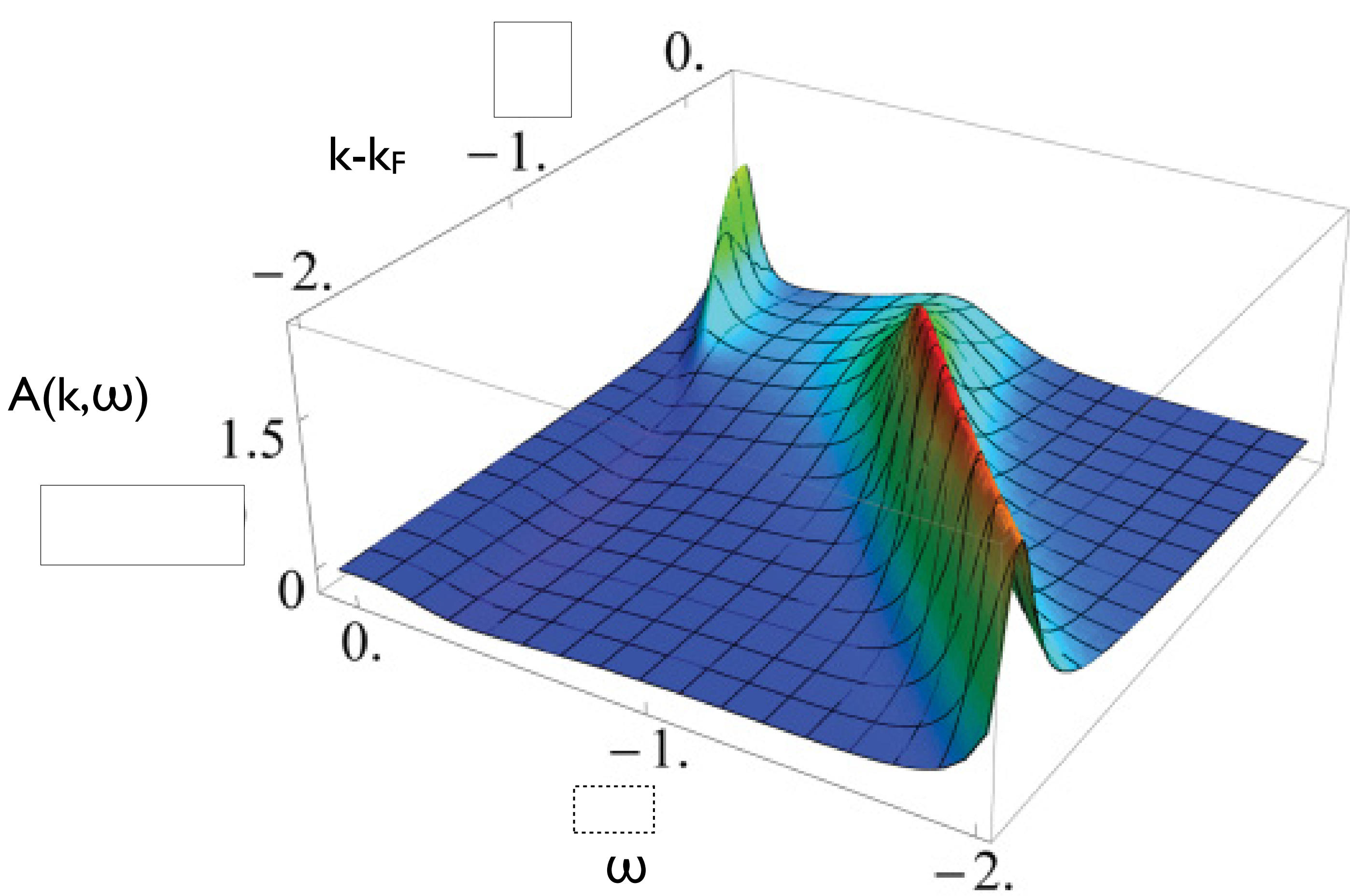

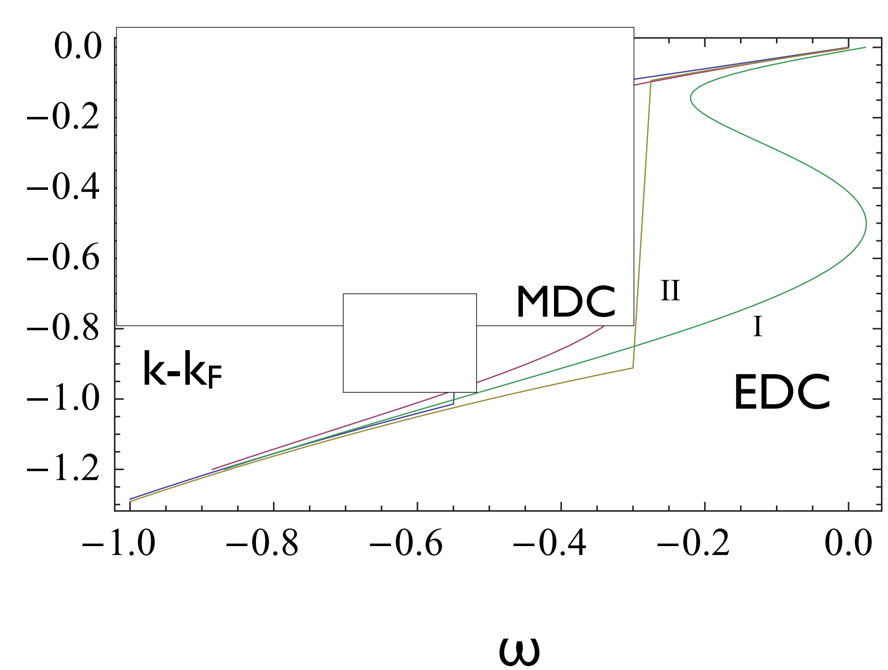

Theoretical Results and Benchmarking

- Short summary of second order results in 2-dimensions
- Comparison with High T expansion results
- Comparison with DMFT
- Comparison with Anderson Impurity Model

Experimental Benchmarking and predictions

- ARPES Line shapes: ECFL
- ARPES Line shapes+ Casey Anderson theory
- ARPES High energy kinks- (t-t'-J model electron doped versus hole doping)
- ARPES Low energy kinks from ECFL

- ASYMMETRY- emergent energy scale- its identification and isolation as an urgent task

Open questions

Short summary of second order results in 2-dimensions

PHYSICAL REVIEW B **87**, 245101 (2013)

Extremely correlated Fermi liquids: Self-consistent solution of the second-order theory

Daniel Hansen and B. Sriram Shastry

$\rho_{\mathcal{G}}(k,\omega) \equiv A(k,\omega)$

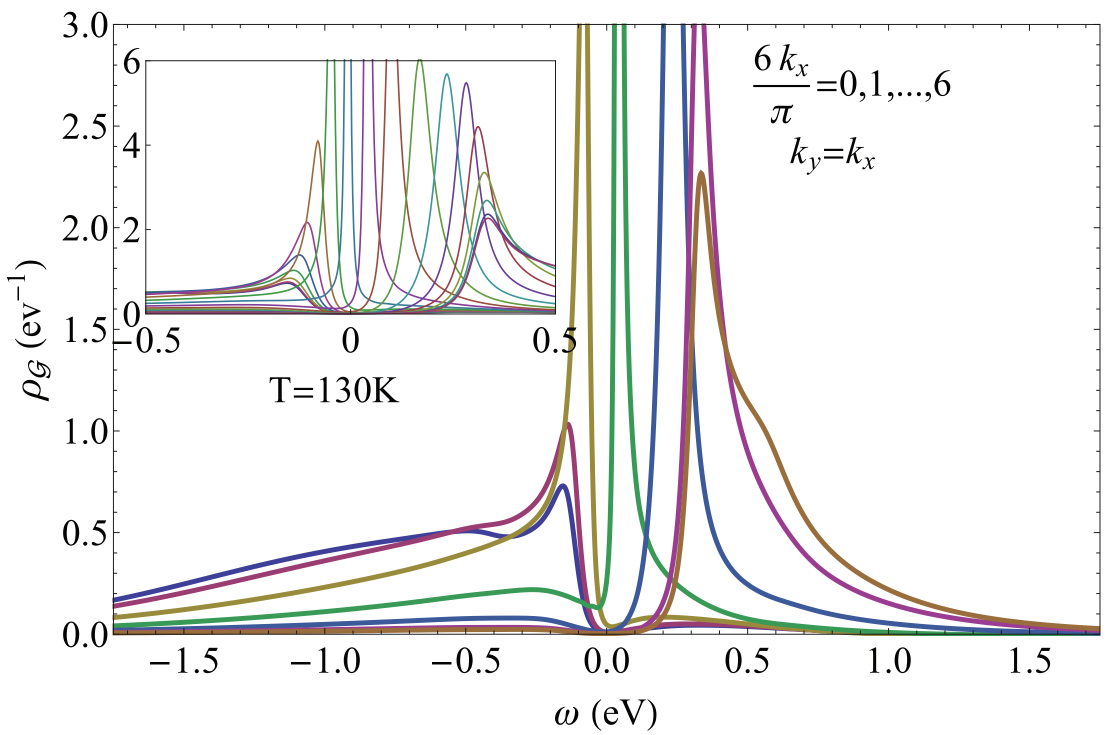

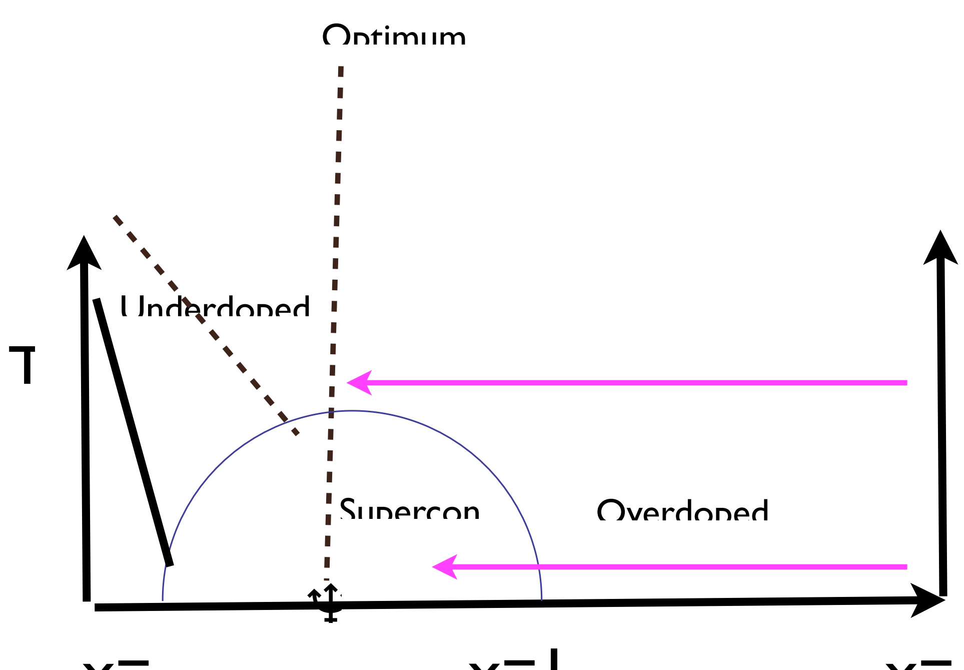

EDC spectra everywhere in Green dots

MDC spectra everywhere in Black dots

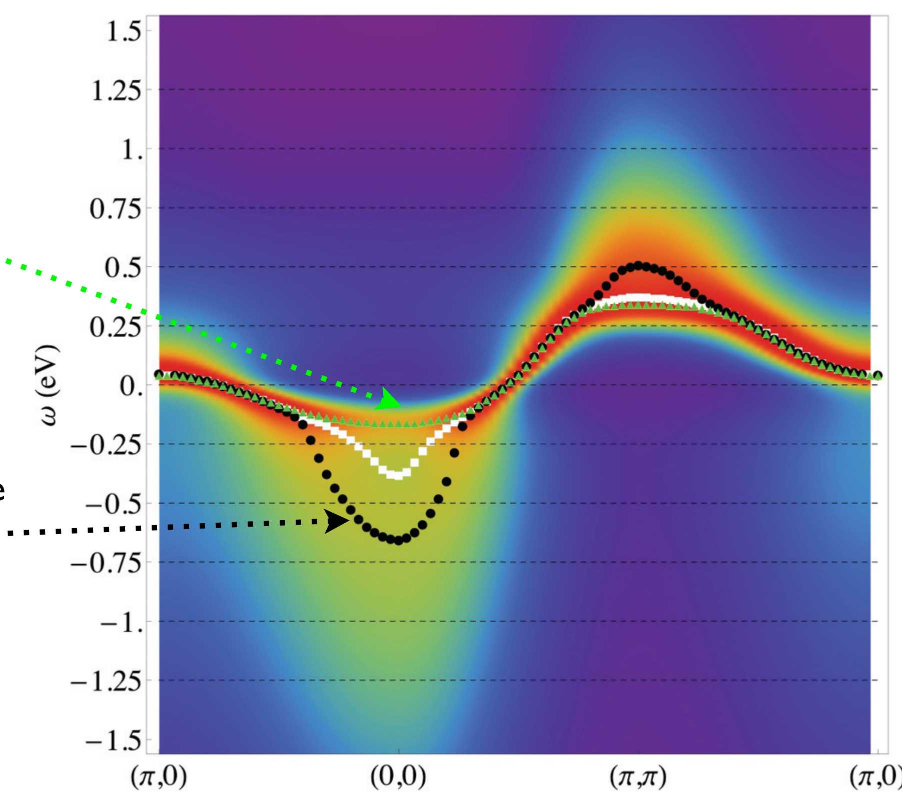

→
Here the electron doped case, modeled by t'/t=-.4 has a larger feature, as in experiments!

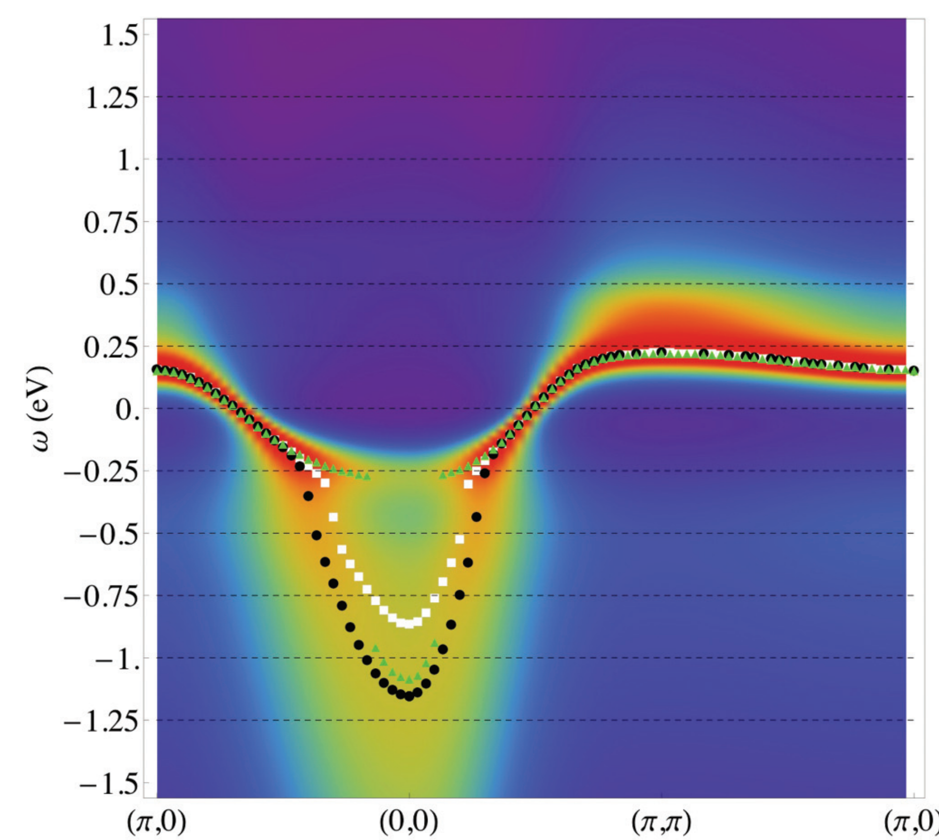

FIG. 3. (Color online) $L = 60$, $(n,T) = (0.75, 300)$ K. Density

Comparison with High T expansion results

PHYSICAL REVIEW B **87**, 161120(R) (2013)

Electronic spectral properties of the two-dimensional infinite-*U* Hubbard model

Ehsan Khatami,[1,2] Daniel Hansen,[1] Edward Perepelitsky,[1] Marcos Rigol,[3] and B. Sriram Shastry[1]

Dynamics out to quite high (8th) order in hopping computed, using Metzner's series for G.

$$\varepsilon_1^0(k) = \frac{\langle\{[\hat{C}(k), H], \hat{C}^\dagger(k)\}\rangle}{\langle\{\hat{C}(k), \hat{C}^\dagger(k)\}\rangle}$$

Symmetric moment (EDC) can be compared with ECFL spectrum to O(λ²), and does quite well except at high energy (unoccupied) states near X point

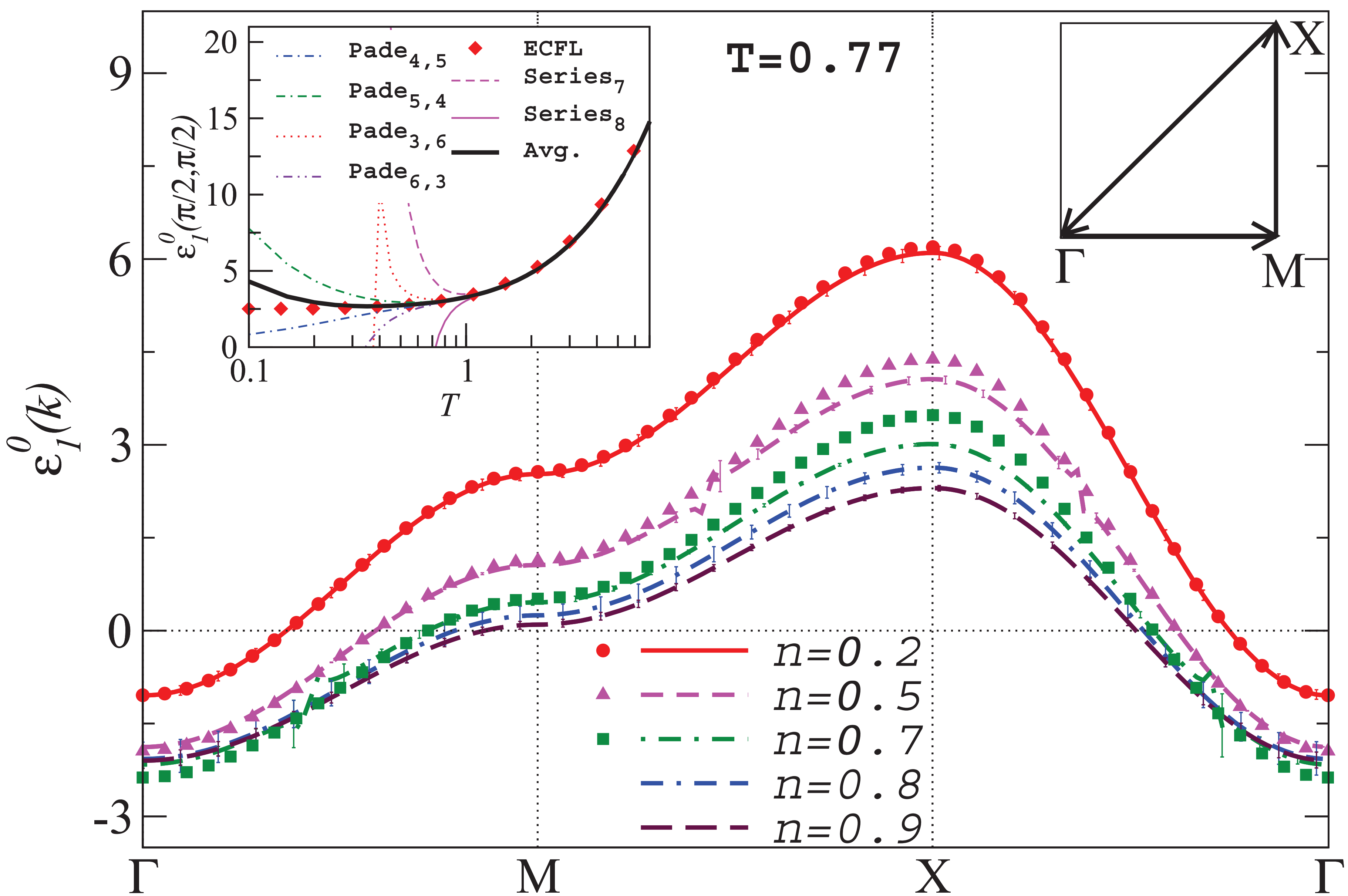

← Here ECFL is the symbols and Pade results as solid/dashed lines- up to n~0.7. Beyond n~0.7 ECFL is not available and only series results are shown.

$$\varepsilon_1^{>}(k) = \frac{\langle [\hat{C}(k), H]\ \hat{C}^{\dagger}(k) \rangle}{\langle \hat{C}(k) \hat{C}^{\dagger}(k) \rangle}$$

Particle addition type moment does much better.
Essentially exact agreement with the actual QP peaks.
Reason is that unoccupied Fermi function invoked here kills the long tails in the occupied side (see ECFL curves), and thereby focuses on the QP's.

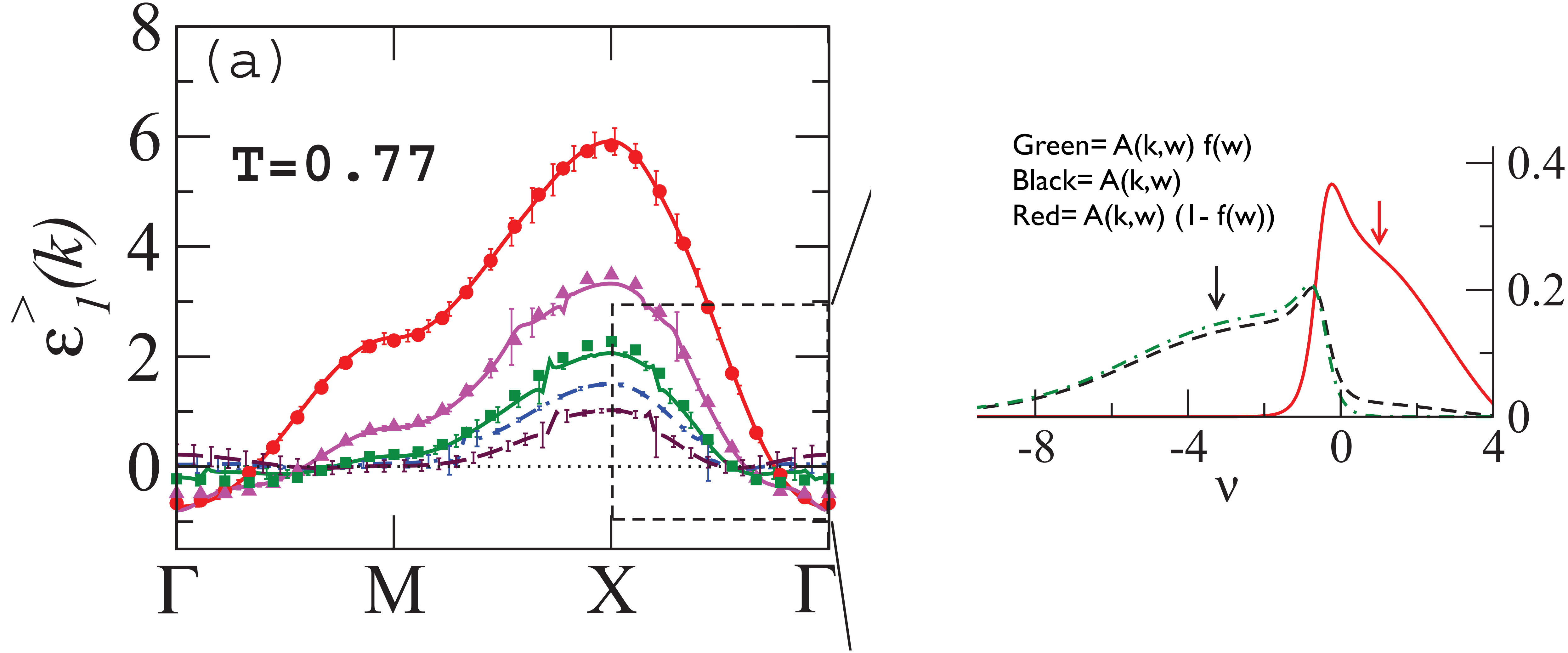

Compare with DMFT in infinite D
Formal preliminaries

Extremely correlated Fermi liquids in the limit of infinite dimensions

Edward Perepelitsky*, B. Sriram Shastry

Annals of Physics 338 (2013) 283–301

- In high dimensions we can show that these are further related through

$$\Psi(k) = \Psi(i\omega_k),$$
$$\Phi(k) = \chi(i\omega_k) + \epsilon_k \Psi(i\omega_k).$$

$$\Sigma_{DM}(k) = \Sigma_{DM}(i\omega_k) = \frac{(i\omega_k + \boldsymbol{\mu})\Psi(i\omega_k) + \left(1 - \frac{n}{2}\right)\chi(i\omega_k)}{1 - \frac{n}{2} + \Psi(i\omega_k)},$$

$$\Psi(i\omega_k) = -\lambda u_0 I_{000}(i\omega_k) + 2\lambda I_{010}(i\omega_k),$$
$$\chi(i\omega_k) = -\frac{u_0}{2}\Psi(i\omega_k) - u_0\lambda I_{001}(i\omega_k) + 2\lambda I_{011}(i\omega_k).$$

$$\mathbf{g}_{\mathrm{loc},m}(i\omega_k) \equiv \sum_{\vec{k}} \mathbf{g}(k)\epsilon_{\vec{k}}^{m},$$
$$I_{m_1 m_2 m_3}(i\omega_k) \equiv -\sum_{\omega_p,\omega_q} \mathbf{g}_{\mathrm{loc},m_1}(i\omega_q)\mathbf{g}_{\mathrm{loc},m_2}(i\omega_p)\mathbf{g}_{\mathrm{loc},m_3}(i\omega_q + i\omega_p - i\omega_k),$$

$$\sum_k \mathbf{g}(k) = \frac{n}{2}; \qquad \sum_k \mathcal{G}(k) = \frac{n}{2}.$$

PHYSICAL REVIEW B **88**, 235132 (2013)

Extremely correlated Fermi liquid theory meets dynamical mean-field theory: Analytical insights into the doping-driven Mott transition

R. Žitko,[1,2] D. Hansen,[3] E. Perepelitsky,[3] J. Mravlje,[1] A. Georges,[4,5,6] and B. S. Shastry[3]

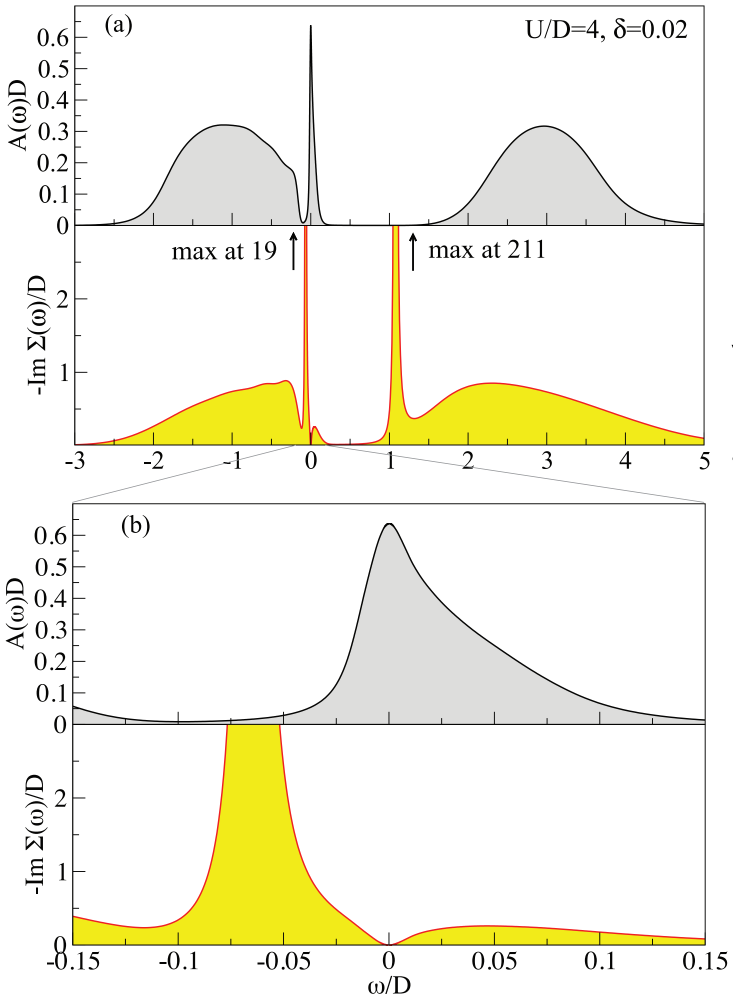

Very high precision low-T DMFT results for local spectral function (k- averged) and Imaginary self energy

Same picture zooming into low ω.

Absolute scale comparison of ECFL and DMFT at different energies.

ε= -D (left) and ε=0 (right).

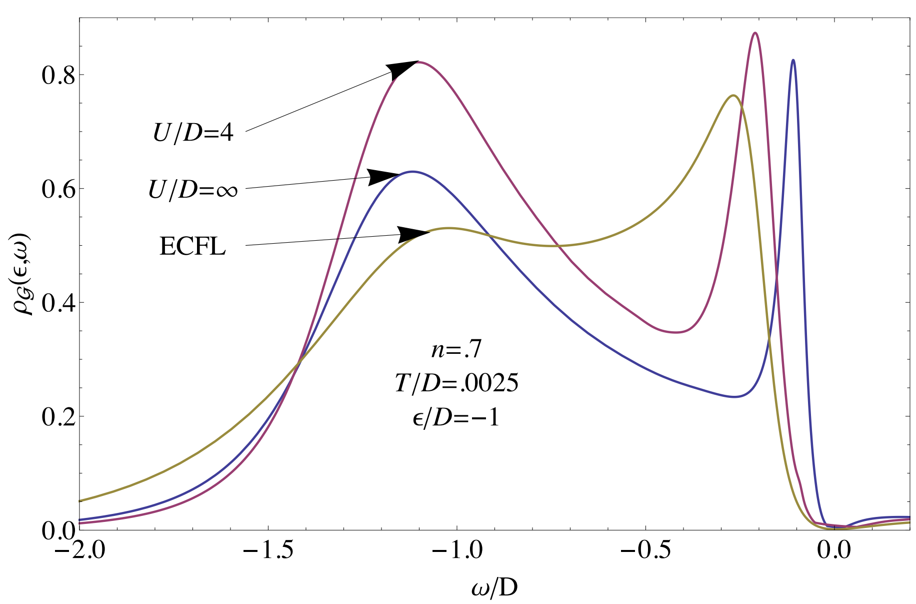

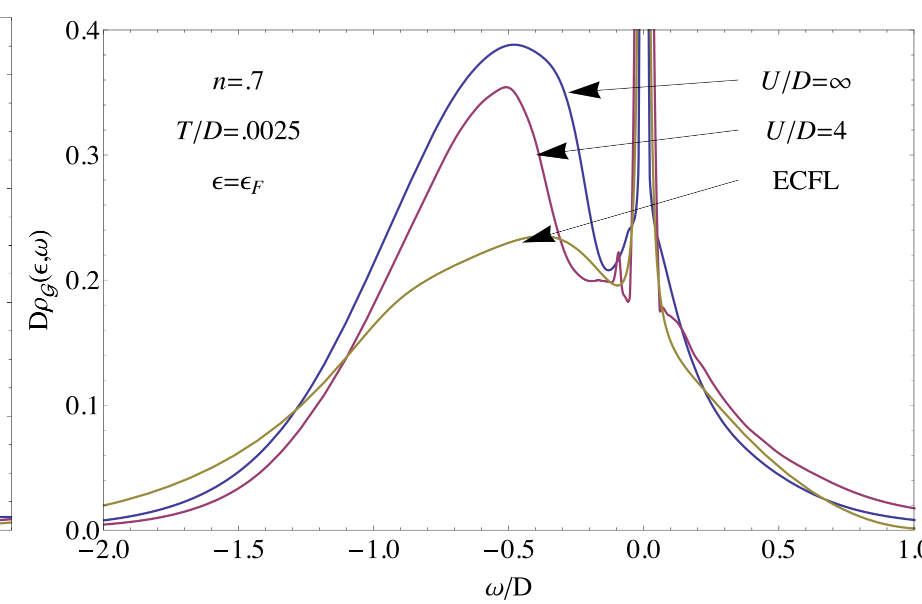

A comparison of ECFL and DMFT spectral function color plots after scaling the frequency by Z (the QP weight). In this rough representation, it is hard to tell the theories apart!

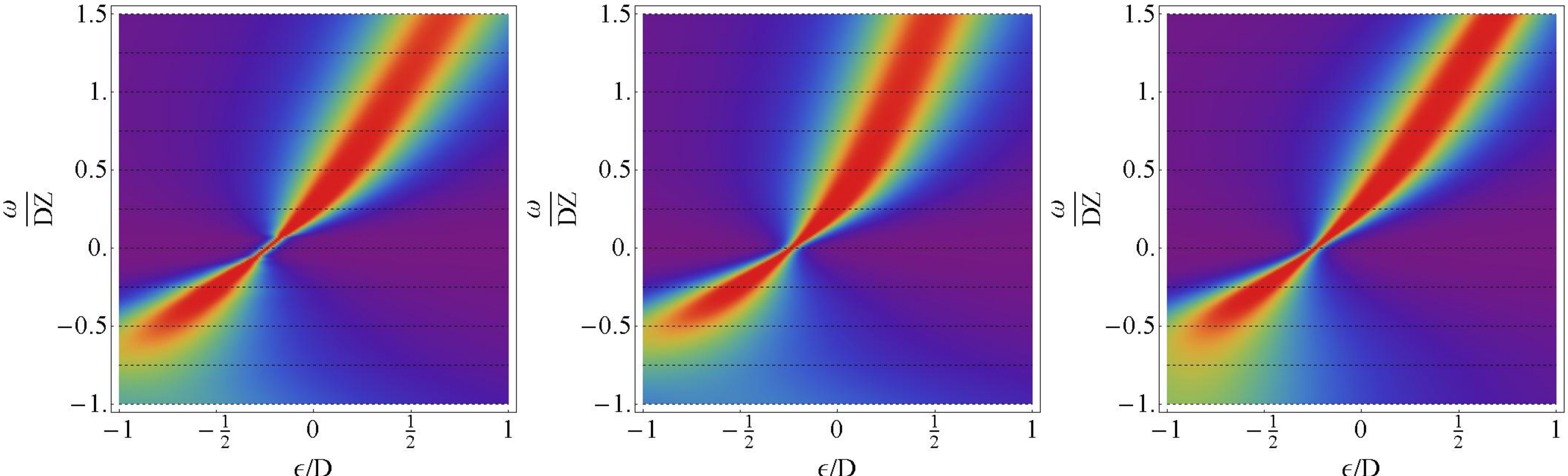

The physical spectral function. From left to right, $U = 4$, $U = \infty$, ECFL with $n = .7$

A comparison of ECFL and DMFT after scaling the frequency by Z (the QP weight).

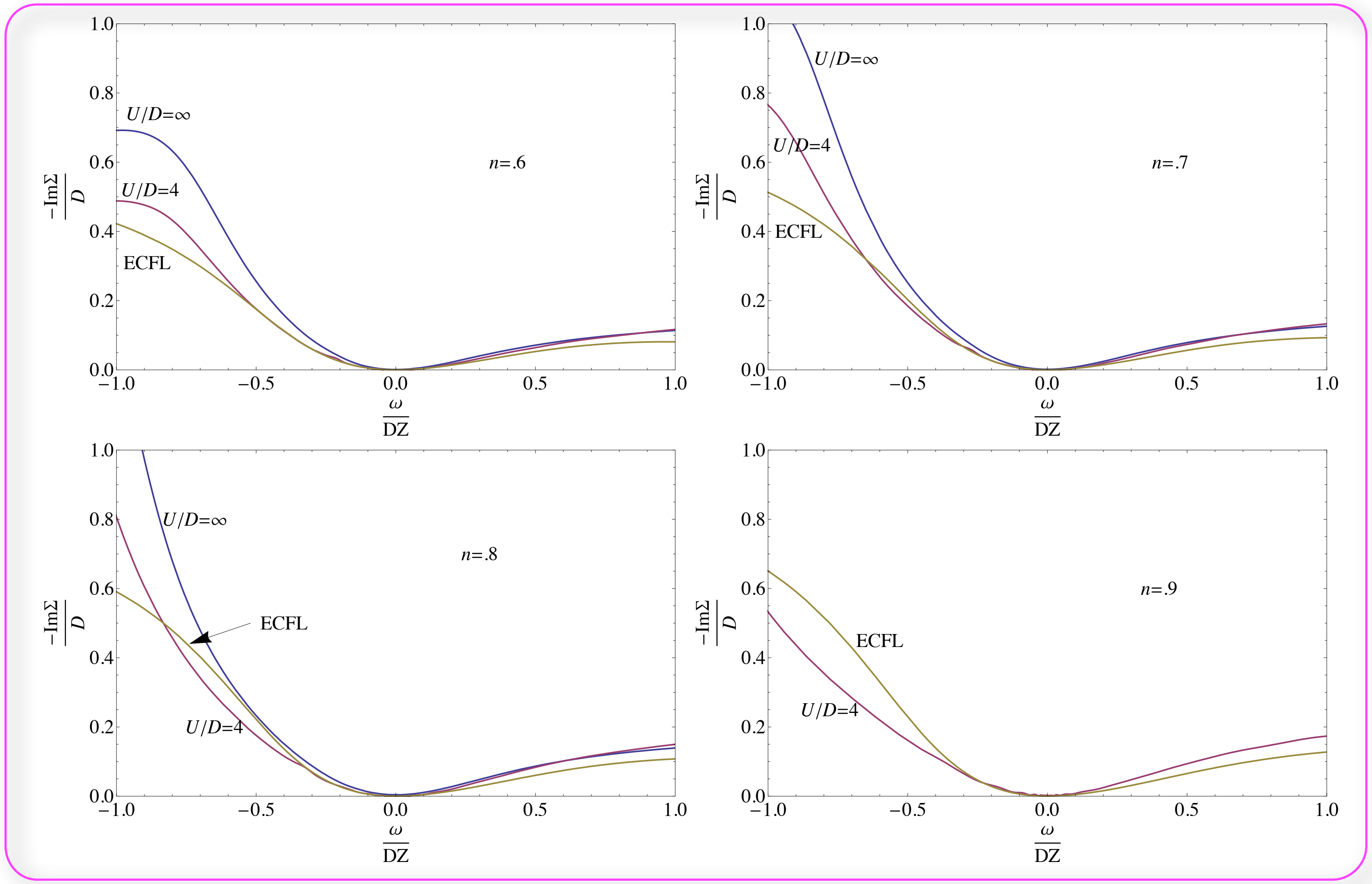

- The $O(\lambda^2)$ version of ECFL used here seems closer to U= 4D, consistent with the interpretation of λ.
- The shapes of the functions are in excellent accord- out to unexpectedly high densities- (ECFL version arguably good for small densities, does impressively well at high densities.)
- Note the strong particle hole assymmetry about ω=0. A strong bias in both theories- discussed later.

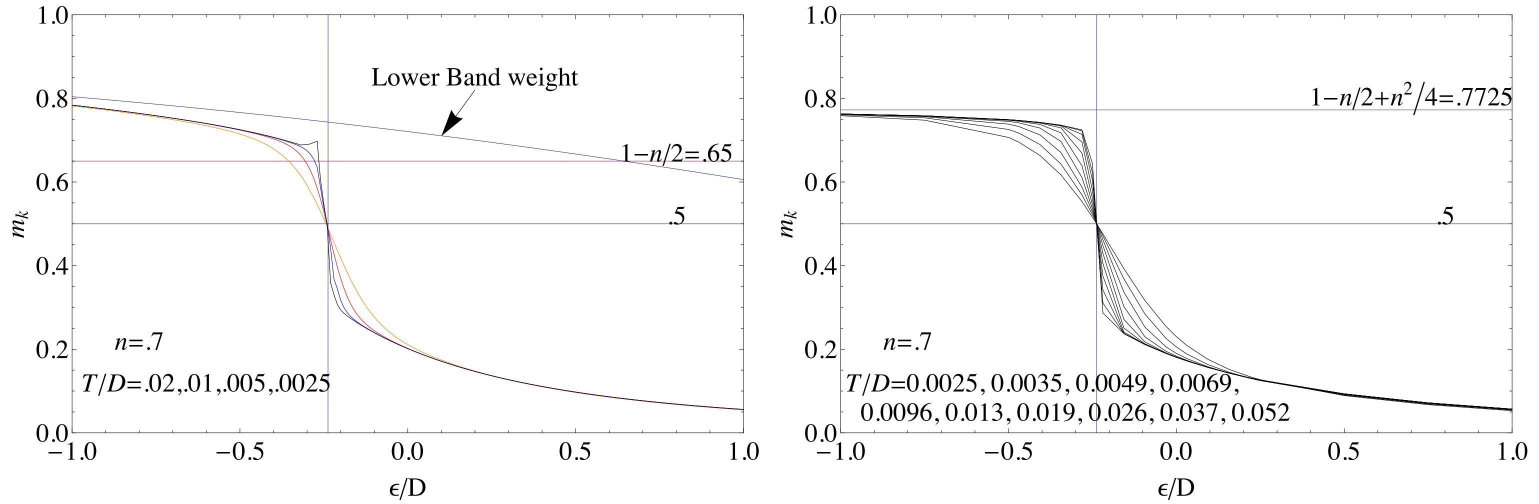

Momentum Occupation vs ε with DMFT and ECFL on left and right, respectively

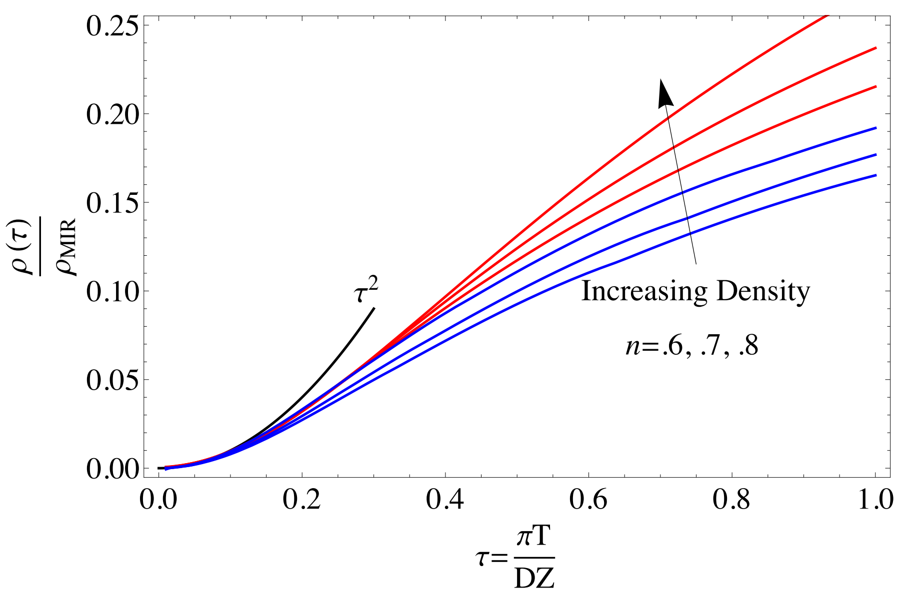

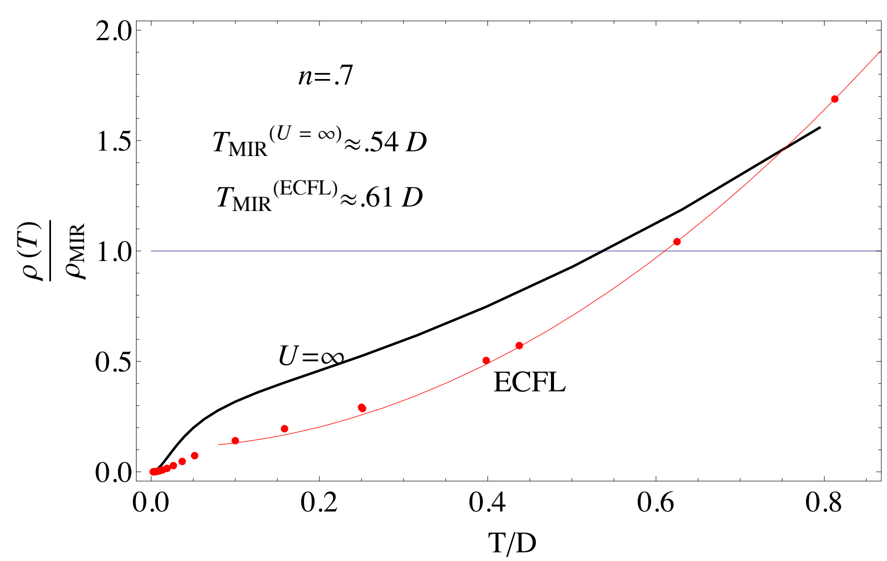

Exciting because we obtain a promising synthesis between the analytical power of ECFL and the exact numerical power of DMFT. Much more to learn from this joint approach.....

Anderson Impurity Model
ECFL at O(λ²) compared to Wilson's Numerical Renormalization Group at infinite U

Extremely correlated Fermi liquid study of the $U = \infty$ Anderson impurity model

B. Sriram Shastry and Edward Perepelitsky Alex C. Hewson

PHYSICAL REVIEW B **88**, 205108 (2013)

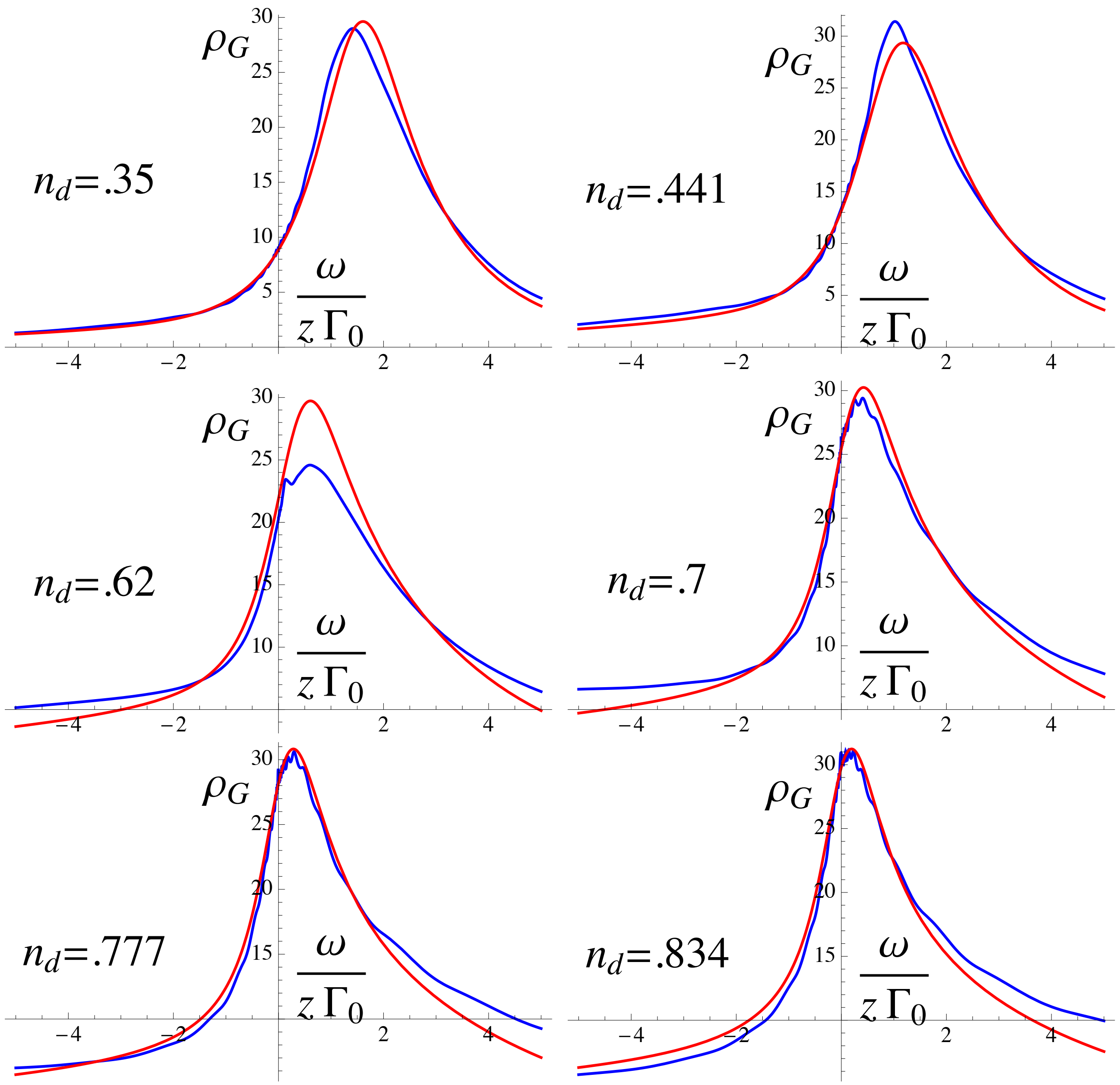

FIG. 1. The spectral density for the physical Green's function versus $\frac{\omega}{\Gamma_0 z}$ for densities of $n_d = .35, .441, .62, .7, .777, .834$. The red curve is the ECFL calculation, while the blue curve is the NRG calculation.

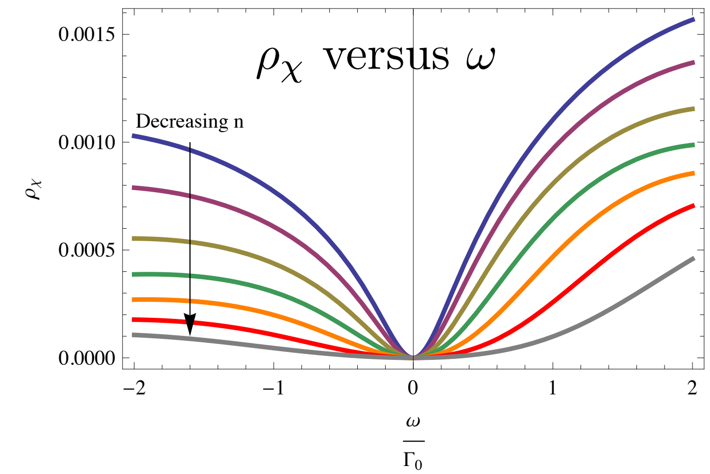

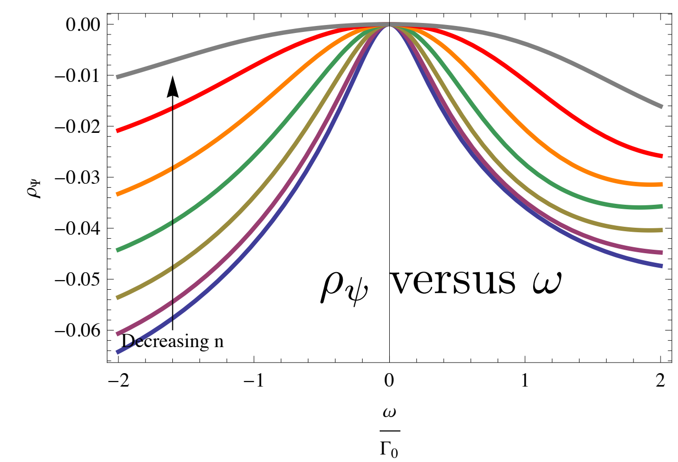

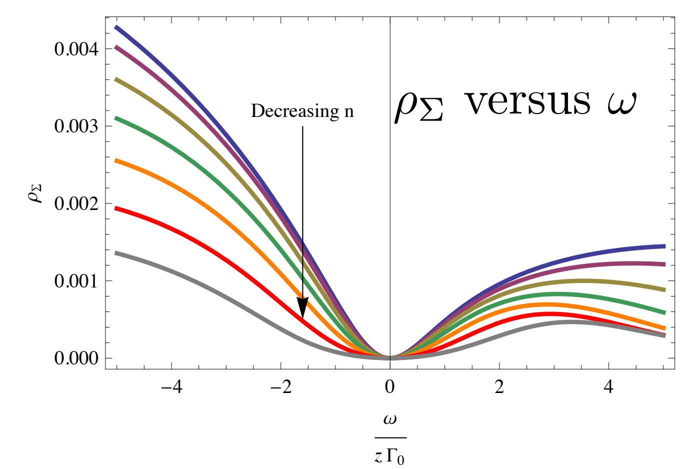

Angle resolved photo emission
ARPES (1990)
Surprising.

$$I_{ARPES} \sim |M|^2 \times A(k,\omega) \times f(w)$$

$$A(k,\omega) = \sum_{\alpha,\nu} e^{-\beta\varepsilon_\alpha} |\langle \nu | C(k) | \alpha \rangle|^2 \; \delta(\omega + \varepsilon_\nu - \varepsilon_\mu)$$

$$A_{FL}(k,\omega) \sim \frac{\Gamma/\pi}{\Gamma^2 + (\omega - E_k)^2}$$

$$\Gamma_{FL} \sim (\omega^2 + \pi^2 T^2)$$

E_k = Quasi hole energy

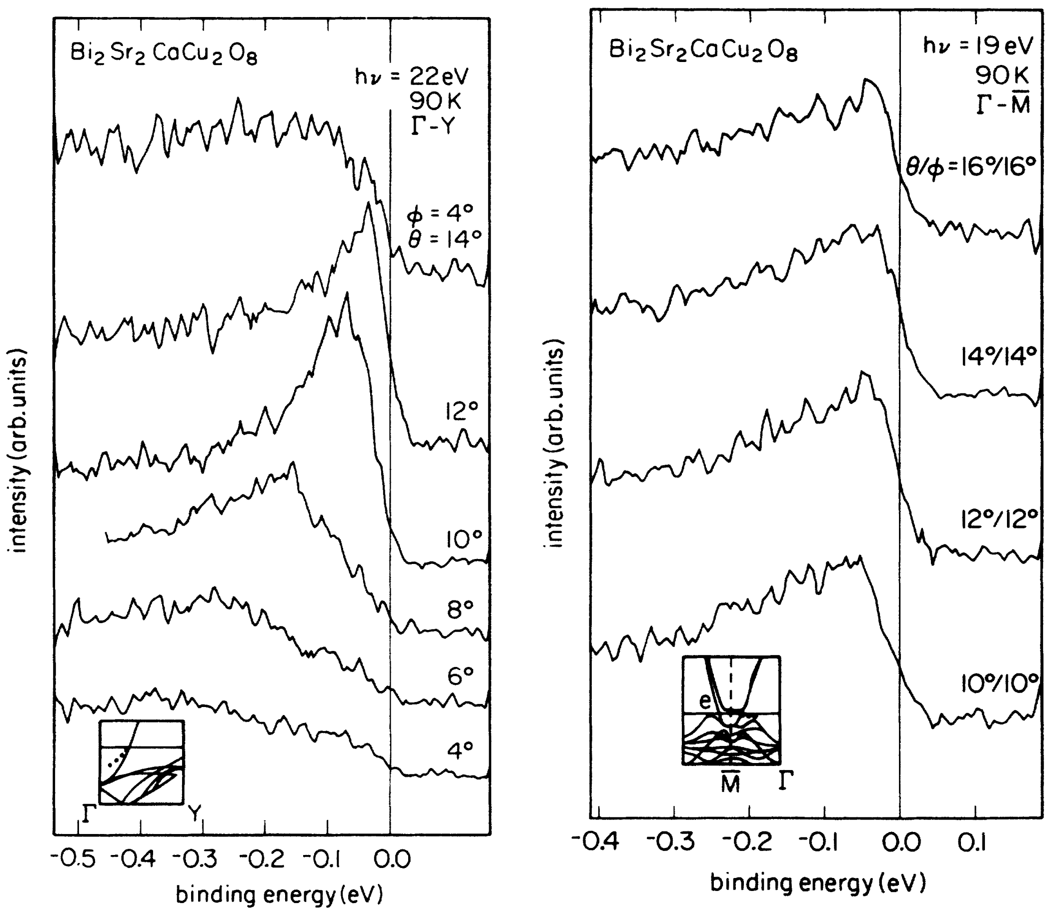

High-resolution angle-resolved photoemission study of the Fermi surface and the normal-state electronic structure of $Bi_2Sr_2CaCu_2O_8$

C. G. Olson, R. Liu, and D. W. Lynch

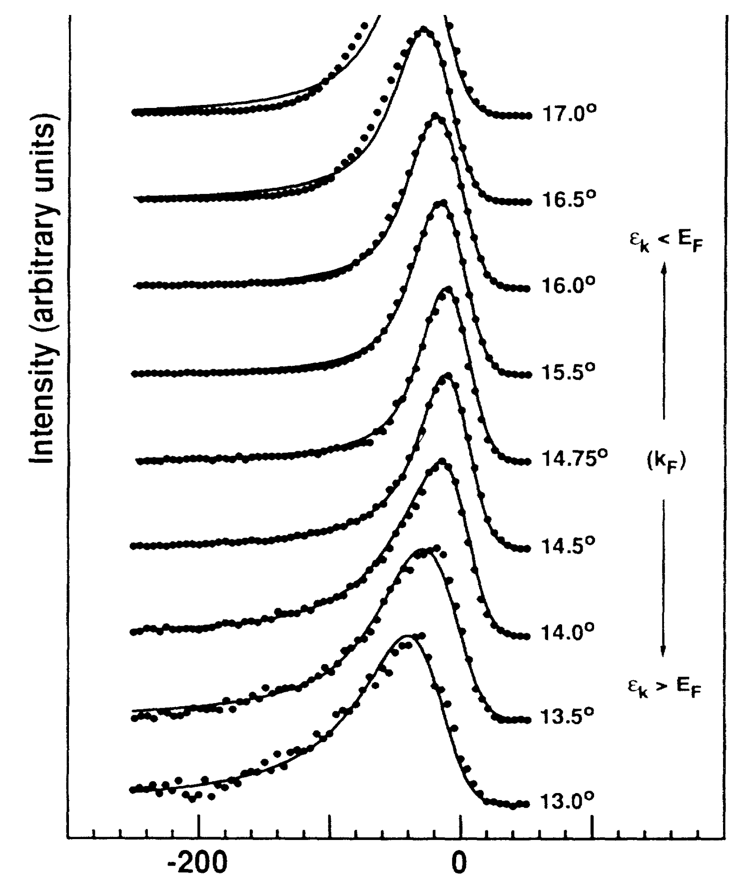

Fermi-Liquid Line Shapes Measured by Angle-Resolved Photoemission Spectroscopy on 1-*T*-$TiTe_2$

R. Claessen, R. O. Anderson, and J. W. Allen
Randall Laboratory, University of Michigan, Ann Arbor, Michigan 48109-1120
C. G. Olson and C. Janowitz

Casey Anderson (2010)
Doniach Sunjic- Nozieres de Dominicis (1968)

P.W. Anderson and P Casey
Hidden Fermi Liquid:
Beautiful and compact idea based on X ray edge singularity work.

LETTERS

Accurate theoretical fits to laser-excited photoemission spectra in the normal phase of high-temperature superconductors

PHILIP A. CASEY[1], J. D. KORALEK[2,3], N. C. PLUMB[2], D. S. DESSAU[2,3] AND PHILIP W. ANDERSON[1]*

$$G(k,\omega)=\int\!\!\int \mathrm{d}x\,\mathrm{d}t\;\mathrm{e}^{i(kx-\omega t)}\,t^{-p}/(x-v_{\mathrm{F}}t).$$

$$=\int \mathrm{d}t\;t^{-p}\mathrm{e}^{i(v_{\mathrm{F}}k-\omega)t}\propto(v_{\mathrm{F}}k-\omega)^{-1+p}.$$

$$p=\frac{1}{4}n^2$$

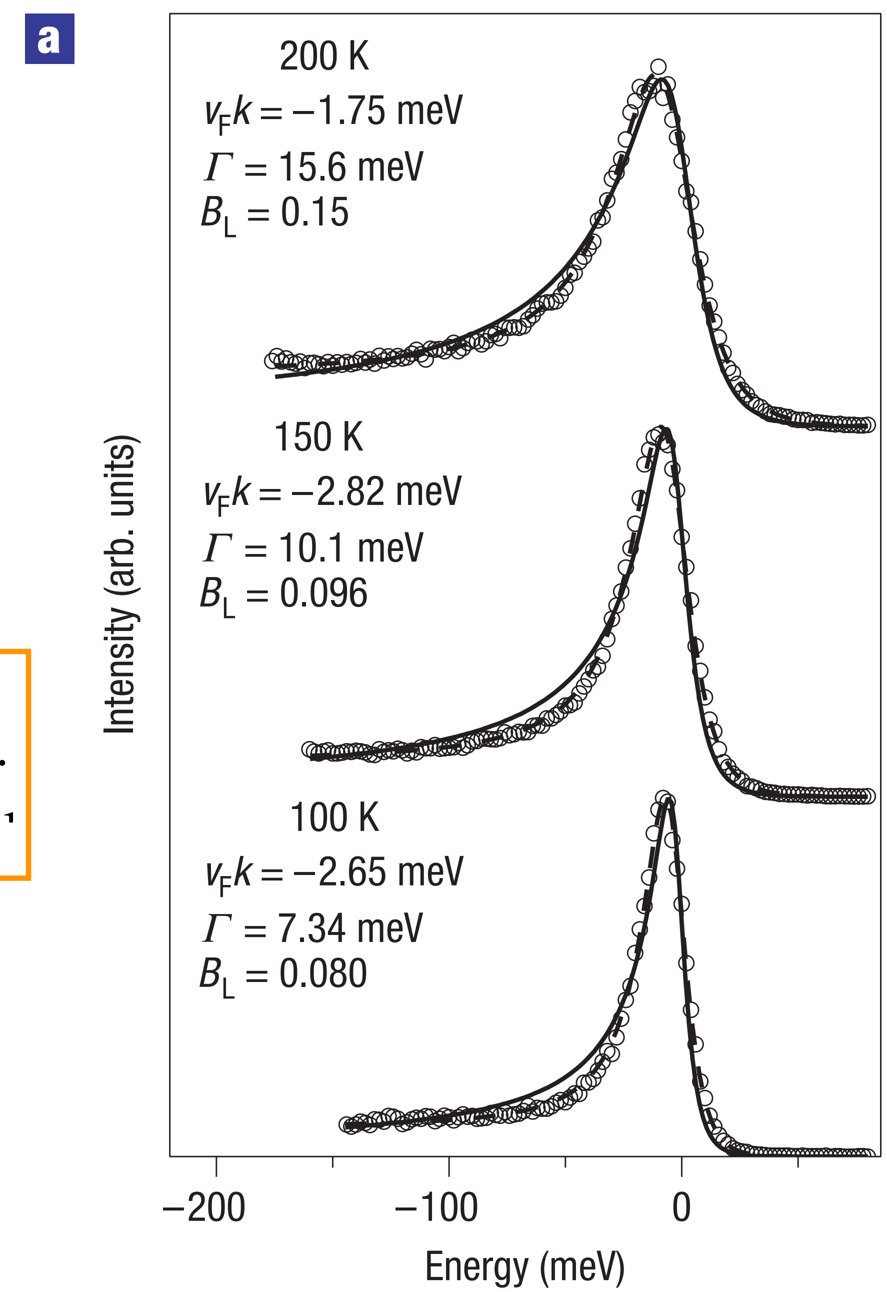

$$A(k,\omega)\;=\;f(\omega/T)\,\frac{\sin[(1-p)(\pi/2-\tan^{-1}[(\omega-v_{\mathrm{F}}k)/\Gamma])]}{[(\omega-v_{\mathrm{F}}k)^2+\Gamma^2]^{(1-p)/2}}.$$

$$\Gamma=aT$$

At T=0 is a Non Fermi Liquid at any density n.
At finite T looks a lot like ECFL because it has the right asymmetry built into it

Simplified ECFL 3 parameter fn vs data:

$$A_{sECFL}(\omega) = \frac{1}{\pi}\frac{\Gamma(\omega)}{\Gamma^2(\omega) + (\omega - \hat{k}v_F - h(\omega))^2} \times (1 - \frac{\omega}{\Delta} + c\hat{k}v_F)$$

$$\Gamma(\omega) = \frac{\omega^2 + \pi^2 T^2}{\omega_0} e^{-(\pi^2 T^2 + \omega^2)/\Omega_0^2}$$

$$\Gamma \rightarrow (\Gamma + \eta)$$

Energy dispersion and the 10 chosen values of k to compare theory and experiment.

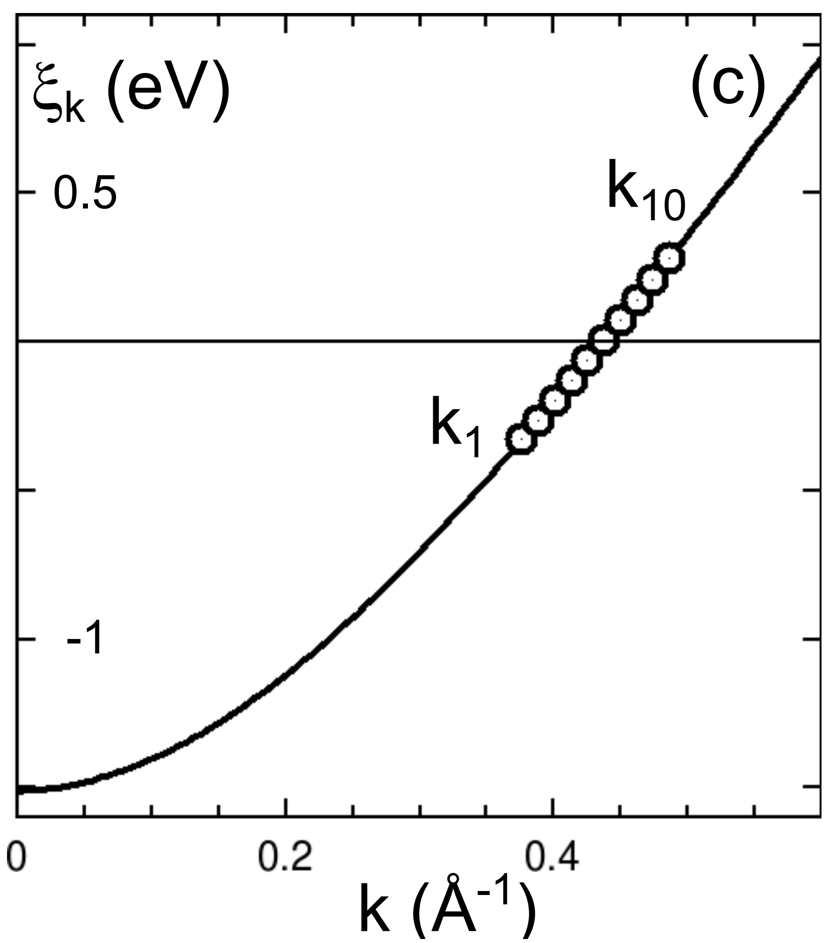

Synchrotron ARPES data from
J Campuzzano's group compared to theory.
BISSCO at optimal doping T= 115K along <11> direction.
Note that η =.12 eV (rather large)

PRL 107, 056404 (2011) PHYSICAL REVIEW LETTERS week ending 29 JULY 2011

Extremely Correlated Fermi-Liquid Description of Normal-State ARPES in Cuprates

G.-H. Gweon,[1,*] B. S. Shastry,[1,†] and G. D. Gu[2]

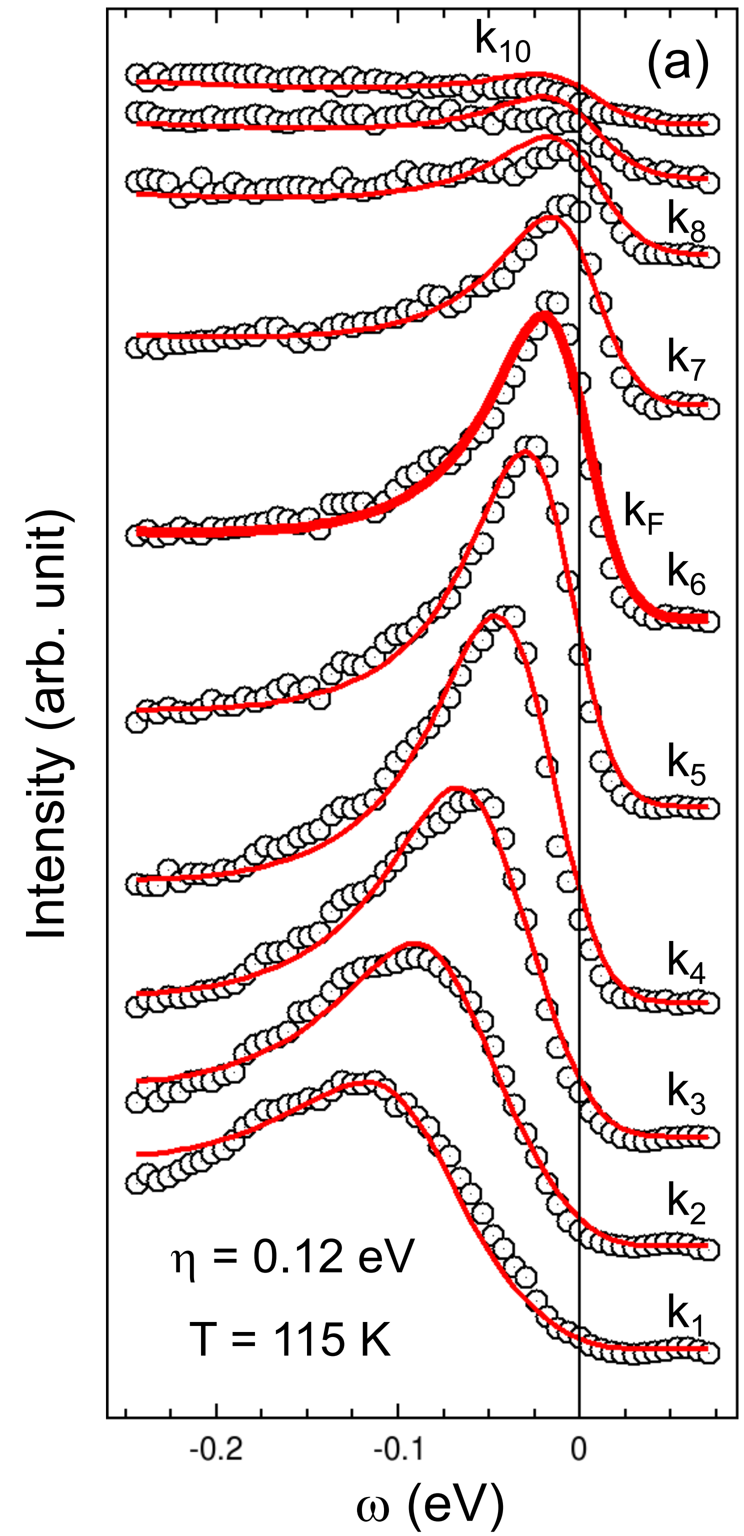

Laser ARPES BISCO 2212

η=.032 eV

Synchrotron ARPES BISCO 2212

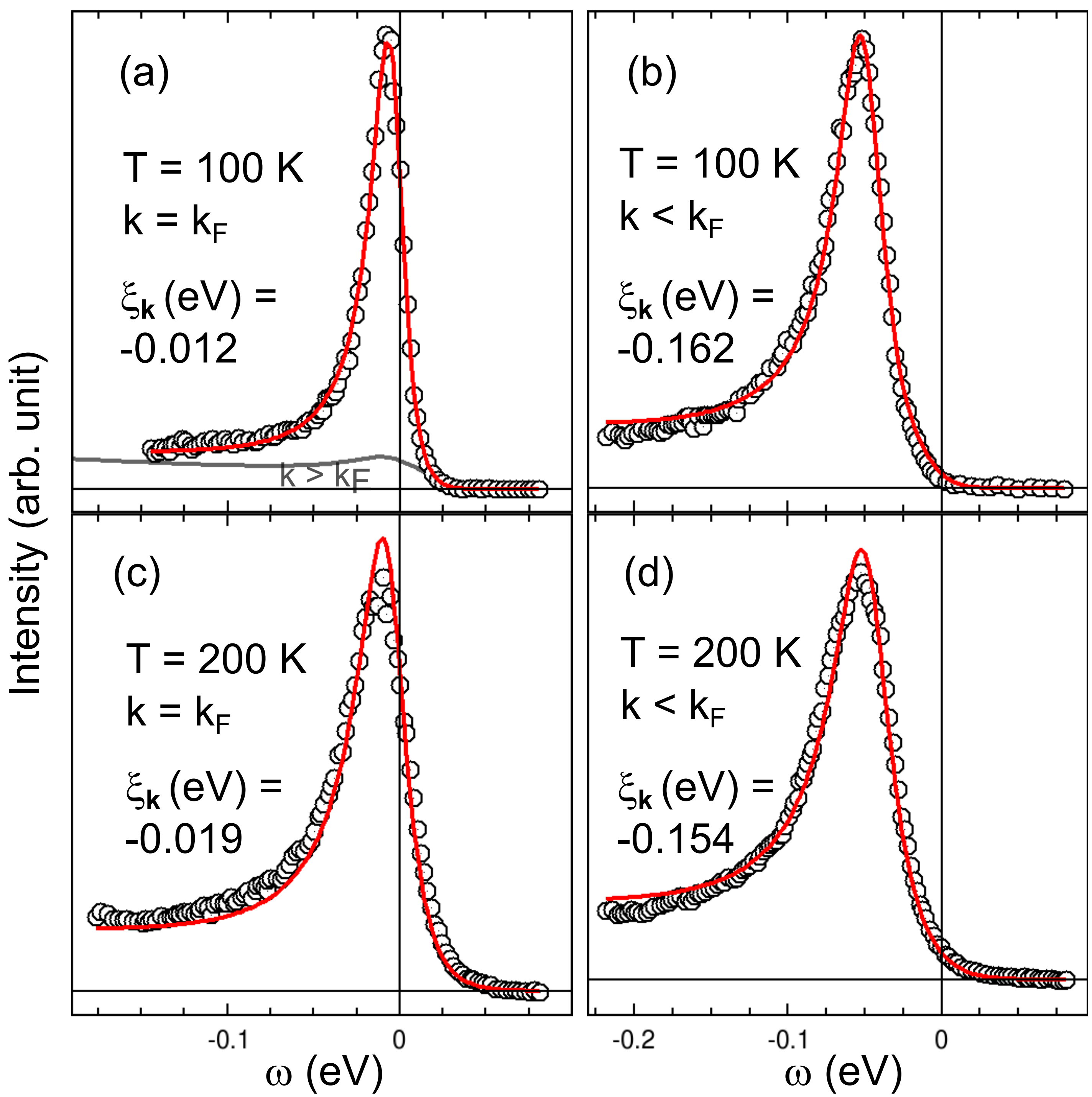

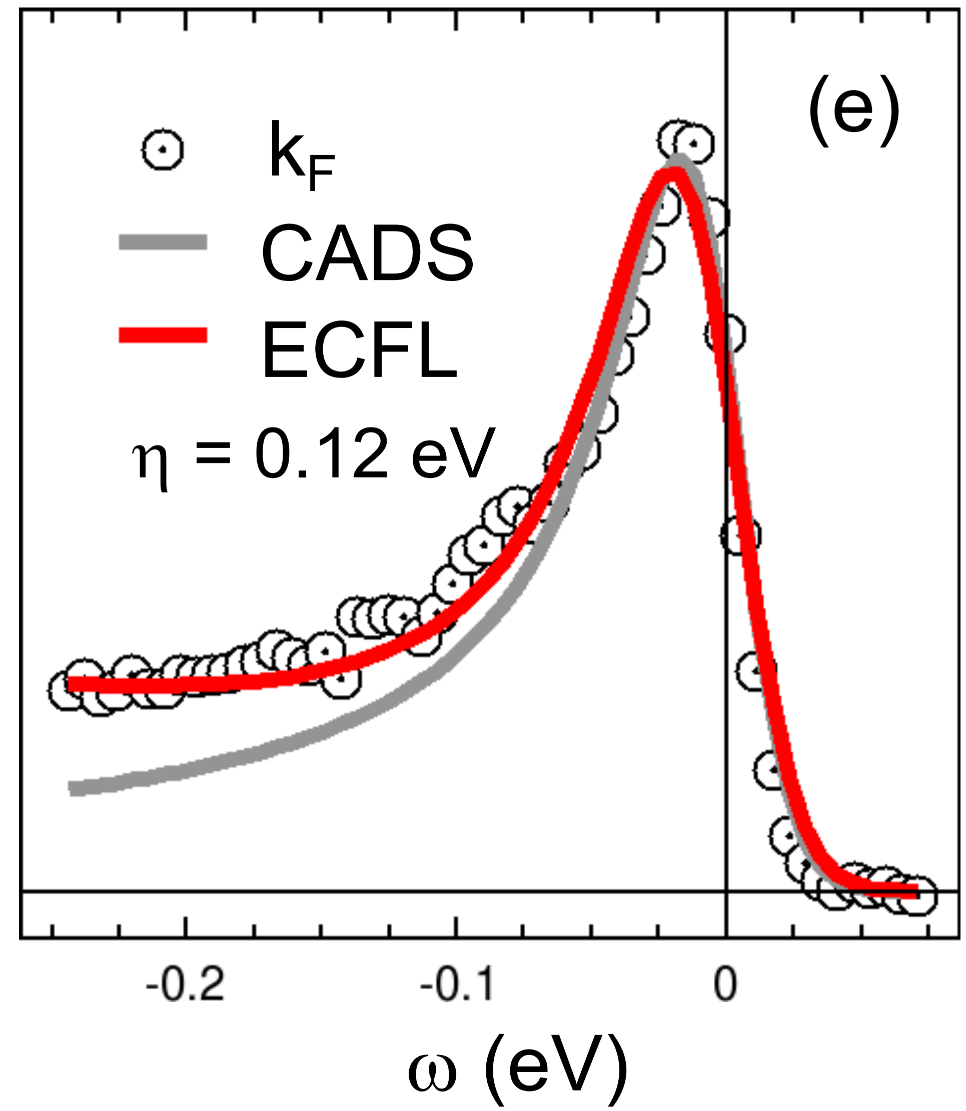

Same physical parameters only η different

- η depends upon initial energy of photon-
- Larger η for surface sensitive probe (HE Synchrotron Arpes)
- small η for bulk sensitive probe (LASER Arpes)

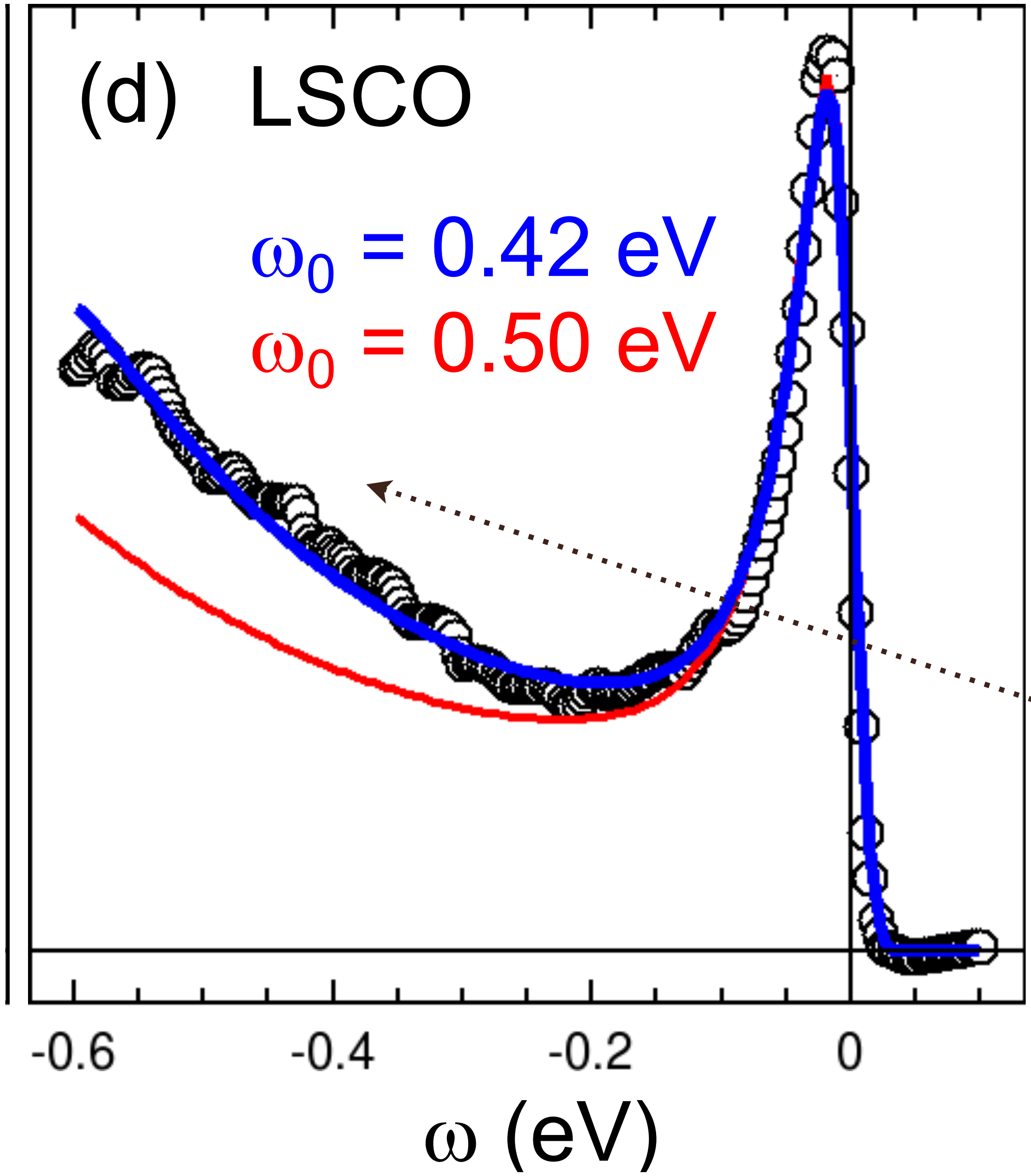

Fujimori, ZX Shen et al

$$A(\vec{k},\omega) = A_{FL}(\vec{k},\omega)\left(1 - \frac{n}{2} + \frac{n^2}{4}\cdot\frac{\xi_{\vec{k}} - \omega}{\Delta_0}\right)_+$$

Smoking gun

Linear rise of intensity for occupied states.

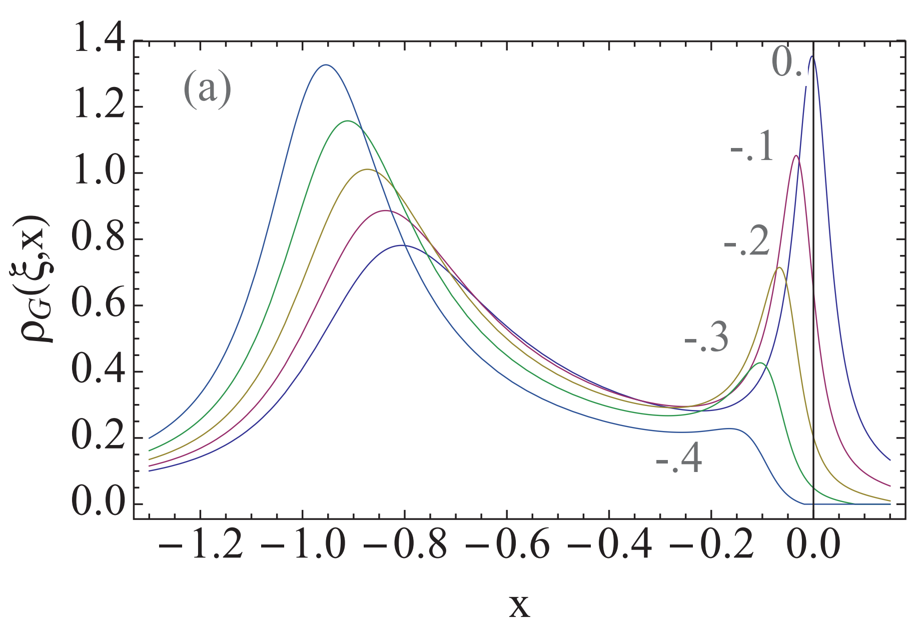

On a larger energy scale there are often broad peaks beyond which the intensity falls.

Phenomenological model for the normal state ARPES line shapes of high temperature superconductors

Kazue Matsuyama[1] and G.-H. Gweon[1,*]

FIG. 4. EDC fits and MDC fits to the data of optimally doped (n = 0.85) LSCO [26], taken along the nodal direction. (a)

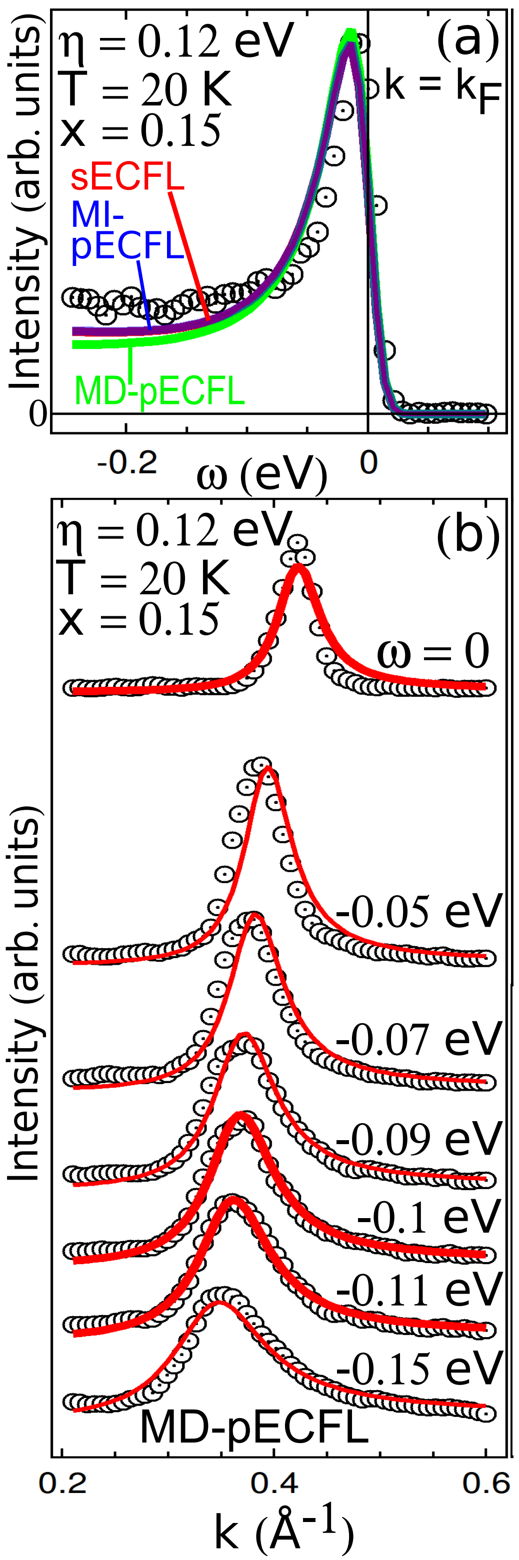

Can we fit
both MDC and EDC's?
Yes-

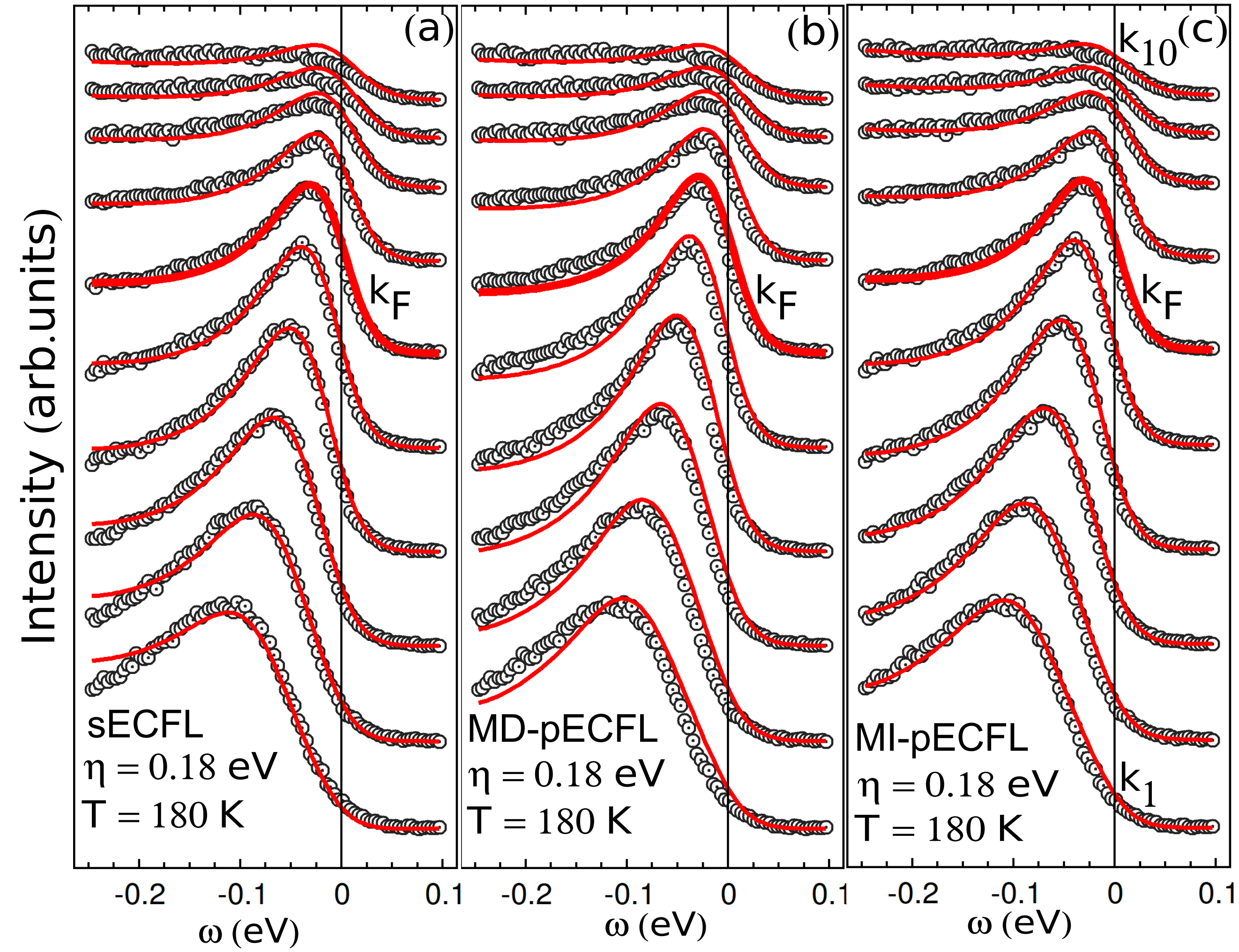

Line shape fits of EDCs for Bi2212 (x = 0.15)

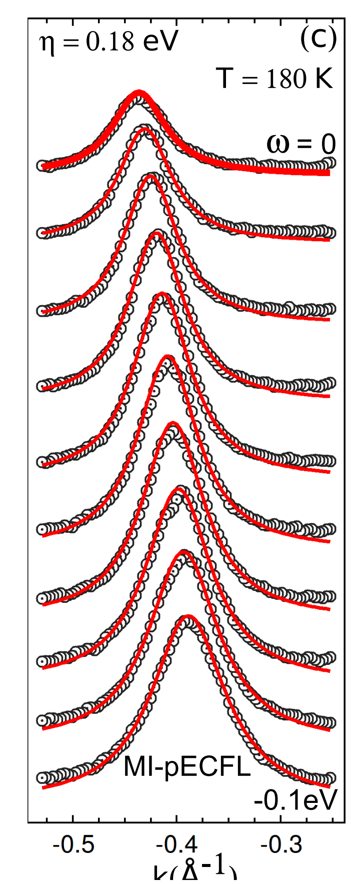

Line shape fits of MDCs for Bi2212 (x = 0.15)

Low energy and High kinks and ECFL

(MDC fits here)

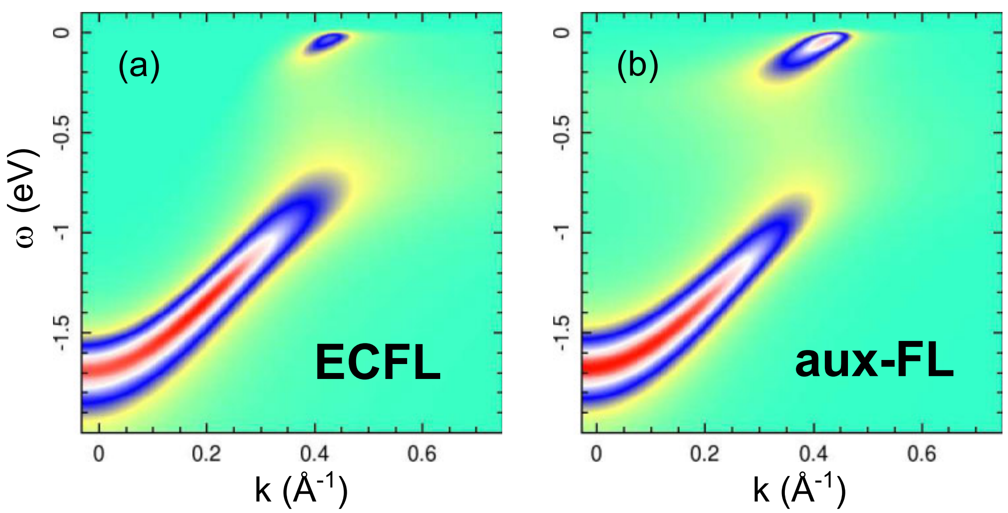

H E Kink in both ECFL and auxiliary FL

L E Kink in ECFL at -.05 eV (not seen in aux-FL)

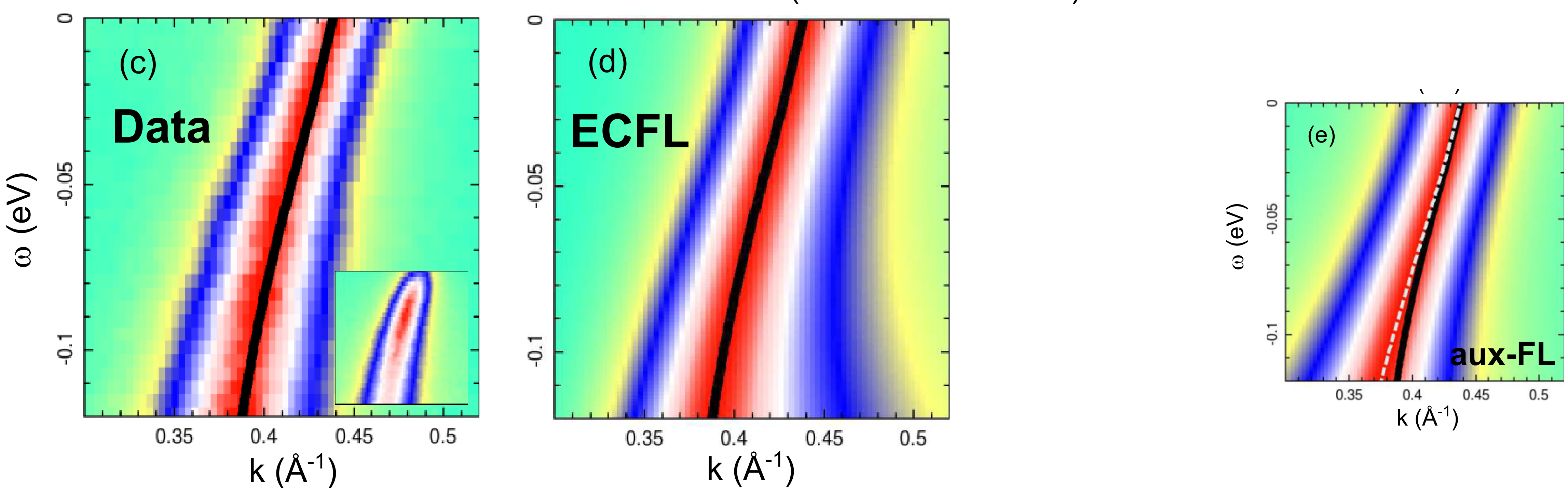

Low energy kinks and their electronic origin. (non Landau FL)

Theory of extreme correlations using canonical Fermions and path integrals
B. Sriram Shastry
Annals of Physics 343 (2014) 164–199

$$A(\vec{k},\omega) = \frac{z_0}{\pi} \frac{\Gamma_0}{(\omega - \nu_\Phi\, \hat{k}\, v_f)^2 + \Gamma_0^2} \times \mu(k,\omega)$$

$$\mu(\hat{k},\omega) = 1 - \frac{\omega}{\Delta_0} + \frac{\nu_0\, \hat{k}\, v_f}{\Delta_0},$$

$$\Gamma_0 = \eta + \frac{\pi^3 (k_B T)^2}{\Omega_\Phi}$$

$$Q(\hat{k}) = \Delta_0 + (\nu_0 - \nu_\Phi)\, \hat{k}\, v_f$$

$$r = \frac{\nu_0}{\nu_\Phi},$$

Q is a momentum variable
r is the ratio of the two velocities ν_0 and ν_Φ.
Recall that Δ_0 is important asymmetry scale.

$$E(k) = \frac{1}{2-r}\left(\nu_\Phi\, \hat{k}\, v_f + \Delta_0 - \sqrt{r(2-r)\,\Gamma_0^2 + Q^2}\right),$$

$$E^*(k) = \left(\nu_0\, \hat{k}\, v_f + \Delta_0 - \sqrt{\Gamma_0^2 + Q^2}\right).$$

$$E^*(k_{kink}) = -\frac{r}{r-1}\Delta_0 - \Gamma_0.$$

$$E(k_{kink}) = -\frac{1}{r-1}\Delta_0 - \Gamma_0\sqrt{\frac{r}{2-r}},$$

Explicit expressions for both kink energies.

E and E* are MDC and EDC peak energies found by max A w.r.t. ω or k.

In MDC a clear maximum is not very robust. EDC more robust

Both spectra are hybrids of massless and massive Dirac spectra,
- asymptotically

$$E(k) \sim \frac{1}{2-r}(\nu_\Phi + (\nu_0 - \nu_\Phi)\, sign(\hat{k}))\, \hat{k}\, v_f.$$

$$E^*(k) \sim (\nu_0 + (\nu_0 - \nu_\Phi)\, sign(\hat{k}))\, \hat{k}\, v_f$$

Both spectra have kinks at Q=0 i.e.

$$(\hat{k}\, v_f)_{kink} = \frac{\Delta_0}{\nu_\Phi(1-r)},$$

Hence kink in occupied side provided r>1.

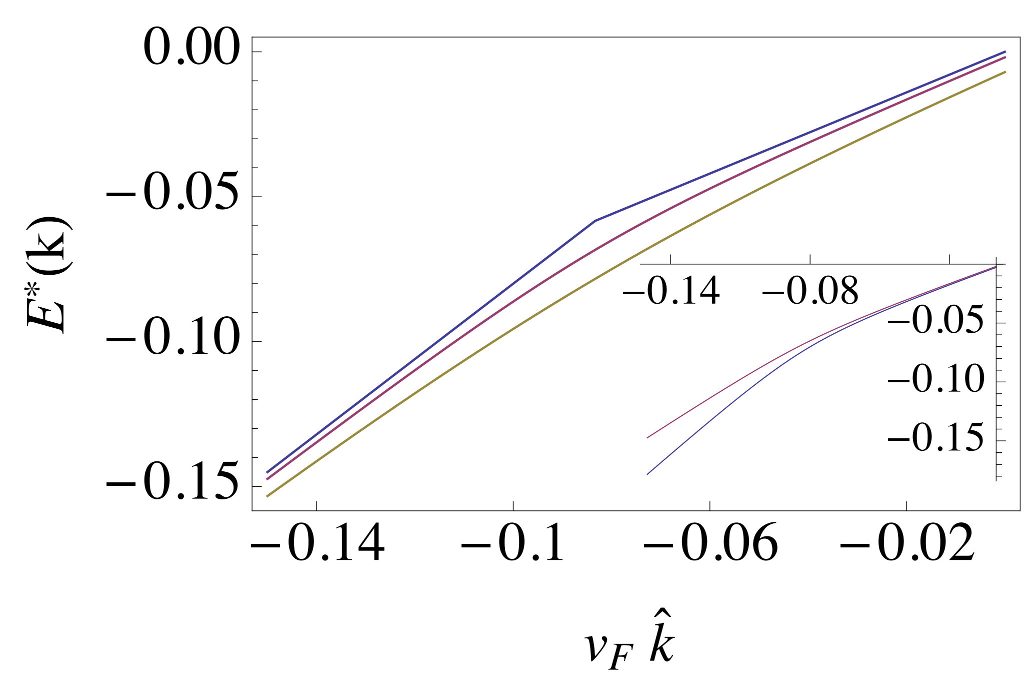

- LE Kink arises from role of caparison function.
- Kink energy reads off important and emergent asymmetry energy sale Δ_0.
- Dependence on n,T and η given explicitly here

Identifying Asymmetry at lowest frequencies in ARPES data:

Main message:

Inverse intensity gives a better perspective for identifying asymmetry.

Intensity itself focusses attention elsewhere.

Doniach Sunjic 1969!!

$$\frac{1}{A(k,\omega)} \quad vs \quad (\omega - E_k^*)^2$$

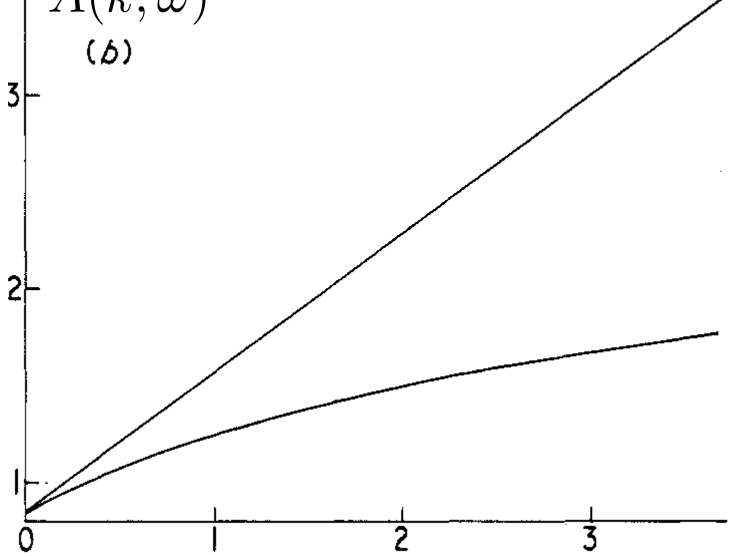

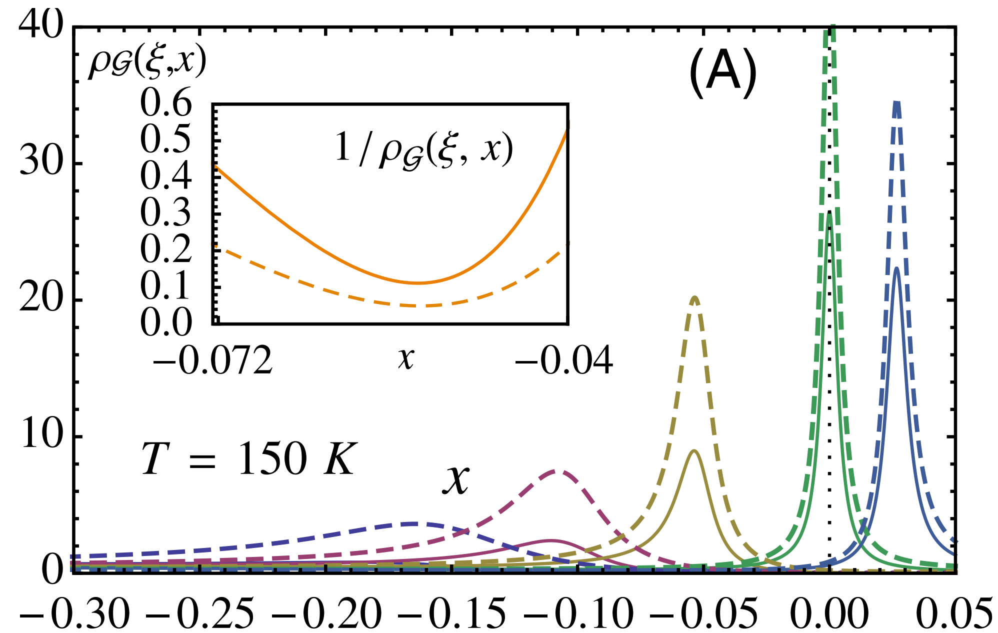

Shastry, Phys. Rev. Letts (2011)

ECFL line shape (and ACDS) predicts that

$$\mathcal{Q}(\widetilde{\omega}_k) \; = \; \frac{\widetilde{\omega}_k^2}{A(k, E_k^*)/A(k, E_k^* + \widetilde{\omega}_k) - 1}$$

$$\mathcal{Q}(\widetilde{\omega}_k) = A - B\,\widetilde{\omega}_k$$

Construct object Q from intensity

$$\widetilde{\omega}_k = \omega - E_k^*,$$

energy shifted by peak position

A sloping Q factor pinpoints and quantifies asymmetry!

Some predictions re asymmetry

Dynamical Particle-Hole Asymmetry in High-Temperature Cuprate Superconductors

B. Sriram Shastry

PRL **109,** 067004 (2012)

Dynamical P-H transformation $(\hat{k} \equiv \vec{k} - \vec{k}_F)$

$$(\vec{\hat{k}}, \omega) \to -(\vec{\hat{k}}, \omega).$$

$$\mathcal{S}_{\mathcal{G}}(\vec{k}, \omega) \equiv f(\omega) f(-\omega) \rho_{\mathcal{G}}(\vec{k}, \omega) = \frac{1}{|M(\vec{k})|} f(-\omega) I(\vec{k}, \omega).$$

This is the Fermi symmetrized spectral function that focuses attention near chemical potential. Here I(k,w) is ARPES intensity and M is dipole matrix element

Construct symmetric and antisymmetric combinations under the above DPH transformation

$$\frac{1}{2}\left[\mathcal{S}_{\mathcal{G}}(\vec{k}_F + \vec{\hat{k}}, \omega) \mp \mathcal{S}_{\mathcal{G}}(\vec{k}_F - \vec{\hat{k}}, -\omega)\right]$$

From these form the (dimensionless) asymmetry ratio R

$$\mathcal{R}_{\mathcal{G}}(\vec{k}_F | \vec{\hat{k}}, \omega) = \mathcal{S}^{a-s}_{\mathcal{G}}(\vec{k}_F | \vec{\hat{k}}, \omega) / \mathcal{S}^{s}_{\mathcal{G}}(\vec{k}_F | \vec{\hat{k}}, \omega)$$

Important ratio
Can experimentally distinguish between two classes of theories.

Simplified ECFL

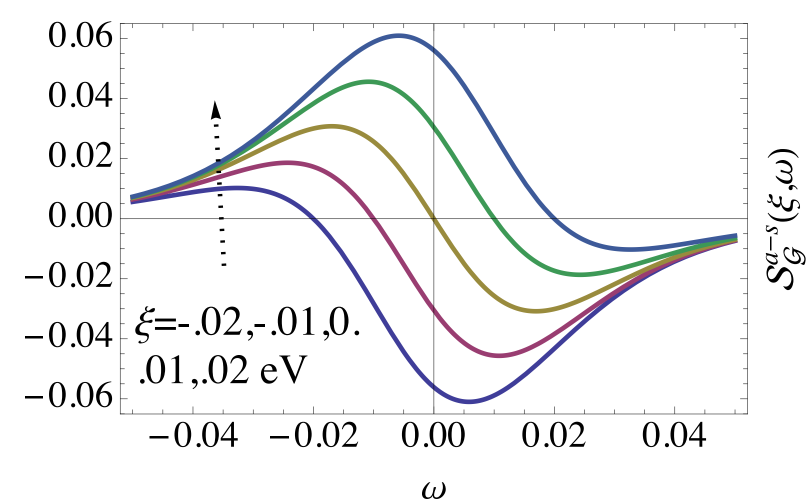

Scale of ω is eV. Enormous asymmetry is

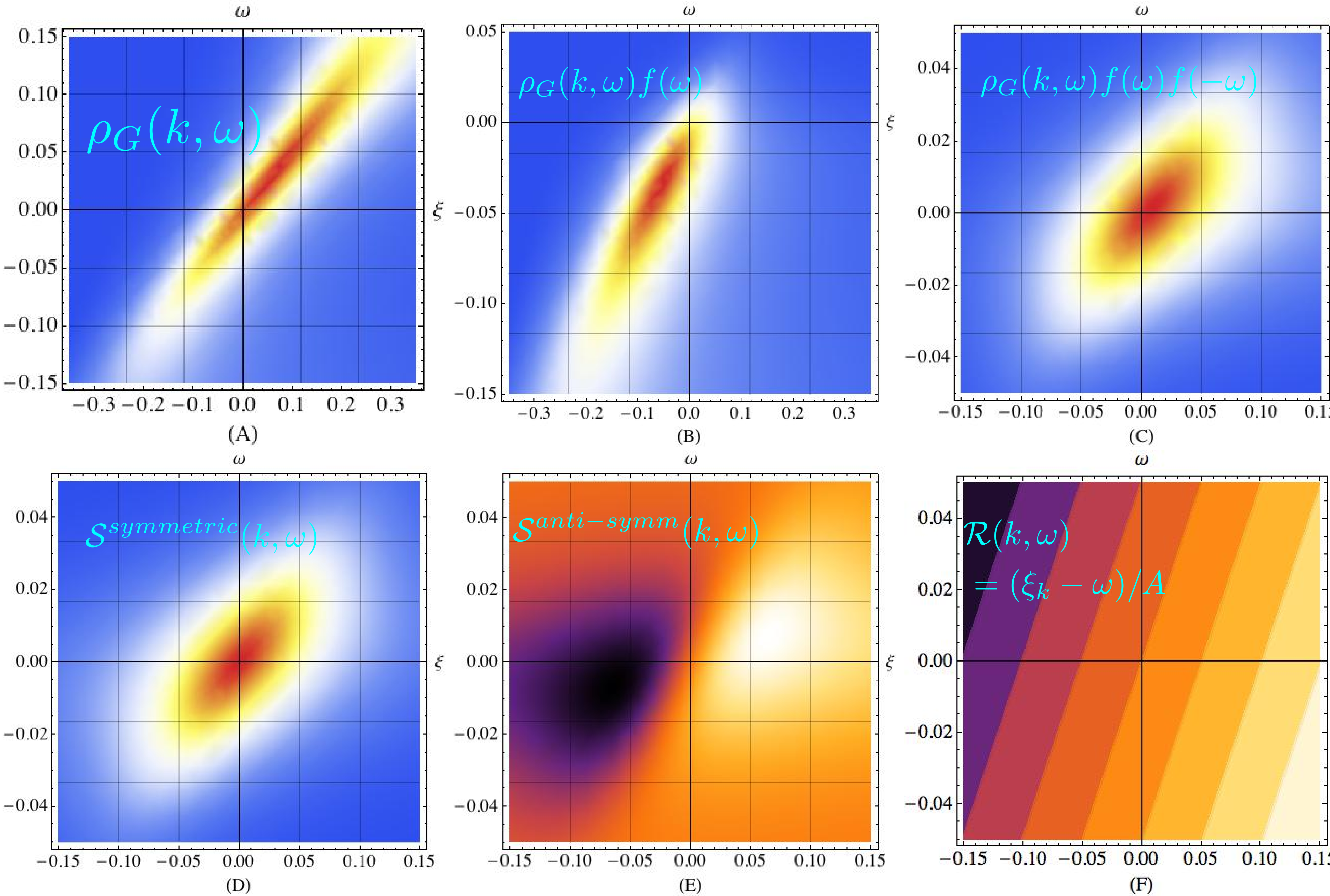

Requires momentum resolution Δk = .001 Angstrom (perhaps just beyond current reach.)

Asymmetry related comments:

- Experimentally feasible if momentum resolution is attained (not too far from current resolution-).
- ECFL and Anderson Casey have similar features. A-C line shapes share the feature of non trivial asymmetry of O(1) on fairly small energy scale (~25 meV). If $\Delta_0 \to (k T)$ then ECFL ~ CADS!
- Fermi liquids do not have such large asymmetries on a similarly small energy scale.
- Marginal Fermi Liquids and Almost AFM Fermi liquids are all particle hole **symmetric**.
- This can be used to discriminate between classes of theories.

Prospects and Open issues

- Superconductivity due to exchange J - this is very natural - (MS in preparation)
- Nature of Mott insulating state?
- Underdoped phase?
- Other broken symmetries (AFM- Quantum liquids..)?

Merci Beaucoup